



From hybridization to introgression between two closely related sympatric ant species

Marion Cordonnier¹ | Thibault Gayet^{2,3} | Gilles Escarguel¹ | Bernard Kaufmann¹

¹UMR5023 Ecologie des Hydrosystèmes Naturels et Anthropisés, CNRS, Université Lyon 1, ENTPE, Université Lyon, Lyon, France

²UMR 5558, Laboratoire de Biométrie et Biologie Evolutive, CNRS, Université Lyon 1, Université de Lyon, Lyon, France

³Unité Cervidés Sangliers, Office National de la Chasse et de la Faune Sauvage, Birieux, France

Correspondence

Marion Cordonnier, UMR5023 Ecologie des Hydrosystèmes Naturels et Anthropisés, CNRS, Université Lyon 1, ENTPE, Université Lyon, Villeurbanne, F-69622, Lyon, France.
Email: marion.cordonnier@hotmail.fr

Funding information

Conseil Départemental de l'Isère; French National Research Agency, Grant/Award Number: ANR-10-LABX-0088 and ANR-11-IDEX-0007

Contributing authors: Thibault Gayet (thibault.gayet@univ-lyon1.fr); Gilles Escarguel (gilles.escarguel@univ-lyon1.fr); Bernard Kaufmann (bernard.kaufmann@univ-lyon1.fr)

Abstract

Interspecific hybridization is becoming more frequent worldwide due to increasing global changes and translocations of organisms. For individual organisms, the most significant negative consequences are sterility or inviability of hybrid offspring. However, hybridization sometimes leads to fertile offspring, promoting introgression from one species into another. In such situations, hybridization can play a key role in evolution and speciation. Combining hypervariable DNA (microsatellites) and mitochondrial DNA markers with the use of several modeling methods allow an efficient detection of hybridization processes. The present study therefore investigates hybridization between two ant species, *Tetramorium immigrans* and *T. caespitum*, using multiple methods, and systematically comparing results with simulated data to ensure accurate identification of hybrids. Introgression was revealed both by backcross detection based on 14 nuclear microsatellite loci and by mitochondrial-nuclear discordance based on comparison with mitochondrial DNA (*cytochrome c oxidase subunit I*). Results were spatially consistent, with hybrids located at latitudes where parental species are sympatric. The causes and consequences of hybridization and introgression between *T. caespitum* and *T. immigrans* remain to be further investigated, especially because *T. immigrans* could be an invasive species in France.

KEY WORDS

Bayesian clustering, interspecific hybridization, introgression, mitochondrial DNA, pavement ant, *Tetramorium*

1 | INTRODUCTION

Hybridization, that is, reproductive interactions between individuals whose lineages show some degree of evolutionary divergence (Brennan et al., 2015; Harrison, 1990), has been demonstrated to be common (Arnold, 1992, 2006; Mallet, 2005). Such interspecific genetic exchanges are becoming even more frequent worldwide due to increasing global changes and translocations of organisms by humans (Allendorf, Leary, Spruell, & Wenburg, 2001; Brennan et al., 2015). Hybridization processes can have negative impacts on species or ecosystems, through loss of biodiversity and ecosystem degradation (Brennan et al., 2015) contributing directly and indirectly to the

extinction of many species (Allendorf et al., 2001). For individuals, the most significant negative consequences of interspecific hybridization may be sterility or inviability of hybrid offspring, explaining that despite hybridization being a common phenomenon, hybrid individuals within a population should be relatively rare (Butler, Peters, & Kronauer, 2018). In some particular cases, however, hybrid offspring are fertile, and hybridization can lead to the introgression of genes from one species into another (Anderson, 1953; Currat, Ruedi, Petit, & Excoffier, 2008; Excoffier, Foll, & Petit, 2009; Patten, Carioscia, & Linnen, 2015; Taylor, Larson, & Harrison, 2015), which could provide new adaptive variations (Brennan et al., 2015), and even rarely lead to "hybrid speciation" (Dejaco, Gassner, Arthofer,

Schlick-Steiner, & Steiner, 2016; Kulmuni, Seifert, & Pamilo, 2010; Mallet, 2007; Schumer, Rosenthal, & Andolfatto, 2014; Schumer et al. 2018). Hybridization can therefore play a key role in the evolution of many plant and animal taxa (Allendorf et al., 2001; Arnold & Kunte, 2017), even if most authors agree on the negative effects of introgressions of non-indigenous into native gene pools (Allendorf & Luikart, 2009; Mallet, 2005).

In view of these consequences of hybridization, its detection is of major importance in ecology and evolution. The accurate detection of putative first-generation (F1) hybrids and backcrosses resulting from hybridization is a critical task. The use of hypervariable DNA markers (microsatellites) and new Bayesian modeling methods have dramatically improved admixture analyses and individual assignment testing (Randi, 2008). Different approaches, implemented in software such as STRUCTURE (Falush, Stephens, & Pritchard, 2003; Pritchard, Stephens, Rosenberg, & Donnelly, 2000), BAPS (Corander & Marttinen, 2006) and NEWHYBRIDS (Anderson & Thompson, 2002), have been used in numerous studies to identify hybrid individuals based on simulated F1 hybrids and backcrosses (Cabria et al., 2011; Sanz, Araguas, Fernández, Vera, & García-Marín, 2009; Steyer, Tiesmeyer, Muñoz-Fuentes, & Nowak, 2018; Vähä & Primmer, 2006). These studies concluded that all these approaches lead to consistent identification of admixed first-generation hybrids and backcrosses. However, STRUCTURE seemed more efficient than BAPS to detect an admixed genotype and to correctly estimate an individual's ancestry composition (Bohling, Adams, & Waits, 2013). Burgarella et al. (2009) found that the use of STRUCTURE resulted in the highest power to detect hybrids, whereas NEWHYBRIDS provided the highest accuracy, and therefore suggested to combine these two complementary Bayesian approaches and to use simulation-based validation to gain resolution in the identification of admixed individuals. More recently, Beugin, Gayet, Pontier, Devillard, and Jombart (2018) compared the performance of the model underlying *Snapclust* with NEWHYBRIDS and suggested that although NEWHYBRIDS recovered more efficiently parental populations, *Snapclust* was not only faster but exhibited improved performances for the identification of hybrids at deeper levels of hybridization (i.e., beyond the first generation of hybrids).

Because mitochondria are usually inherited from the mother, recurrent backcrossing of hybrid females with males from another lineage will ultimately lead to offspring with introgressed mitochondria, that is, mtDNA from the maternal lineage and nuclear DNA from the paternal lineage (Darras & Aron, 2015). The sharing of mitochondrial haplotypes between sympatric, but genetically divergent lineages is therefore the signature of mitochondrial introgression. According to the review of Toews and Brelsford (2012), when foreign mtDNA haplotypes are found deep within the distribution range of a second taxon, those mtDNA haplotypes are more likely to be at a high frequency and are commonly driven by sex-biased asymmetries (e.g., male-biased dispersal, mating behavior or sex-biased offspring production) or adaptive introgression. Combining microsatellite markers and mtDNA should help improve discrimination between situations with only F1 hybrids and situations with introgression.

Such mtDNA and nuclear DNA marker combinations have promoted the detection of hybridization and introgression processes in various organisms. In many ant taxa, hybridization is common and sometimes leads to the evolution of reproductively isolated new lineages (Feldhaar, Foitzik, & Heinze, 2008). The consequences of hybridization in social Hymenoptera could differ from other species as most of the potential deleterious effects could be mitigated by haplodiploidy and eusociality (Butler et al., 2018). However, in many cases, hybridization in ants appears as an evolutionary dead end given that fertile hybrids are rarely found (Feldhaar et al., 2008; Purcell et al., 2016). In such situations, hybrid zones are "tension zones" reflecting a balance between migration and selection against hybrids (Barton & Hewitt, 1989). Nevertheless, these hybrid zones can also be maintained without selection against hybrids, for example, thanks to increased fitness of hybrids along narrow ecotones or to an equilibrium between migration and selection acting along an environmental gradient (Endler, 1977; Moore, 1977). The consequences for gene exchange between species therefore make hybrid zones privileged places for studying the processes of divergence between lineages, as well as the mechanisms limiting genetic exchanges that can lead to speciation or, conversely, the fusion of differentiated species (Harrison, 1990). The few situations providing evidence of introgression, including the case studied here, may therefore provide a powerful way to investigate speciation in social insects (Purcell et al., 2016).

The present study focuses on two ant species of the *Tetramorium caespitum* complex: *T. immigrans* Santschi, 1927 and *T. caespitum* (Linnaeus, 1758; Wagner et al., 2017). Wagner et al. (2017) suggested recent hybridization as source for mitochondrial-nuclear discordance found in two individuals with a *Tetramorium immigrans* mtDNA and which clustered with *T. caespitum* for Amplified Fragment-Length Polymorphism. Cordonnier, Bellec, Dumet, Escarguel, and Kaufmann (2019) identified 285 individuals simultaneously associated with several species based on their genotypes, most of whom had an intermediate genotype between *T. immigrans* and *T. caespitum*. All these individuals with an intermediate genotype could not be assigned to a species in Cordonnier et al. (2019) and were therefore excluded from the analyses. In view of the results of Wagner et al. (2017), these individuals might be hybrids between *T. caespitum* and *T. immigrans*, which would suggest a relatively frequent hybridization between these two species. So far, hybridization between *T. caespitum* and *T. immigrans* has never been studied; it is currently suspected only through the two mitochondrial-nuclear discordances found by Wagner et al. (2017). We investigate here hybridization patterns between *T. immigrans* and *T. caespitum*. More precisely, the study aims to assess if *T. immigrans* and *T. caespitum* do hybridize, and if hybrids are fertile. To detect potential introgression, we used both backcrosses detection based on nuclear DNA (14 microsatellites loci) and mitochondrial-nuclear discordance based on comparison with mtDNA (*Cytochrome C Oxidase subunit I—COXI*). We combined methods implemented in STRUCTURE, NEWHYBRIDS, and *Snapclust* and compared putative hybrids with simulated F1 hybrids and backcrosses. We subsequently compared the range limits of the

detected hybrids to the ranges of parental species in order to validate the spatial consistency of our results.

2 | MATERIAL AND METHODS

Tetramorium immigrans Santschi, 1927 and *T. caespitum* (Linnaeus, 1758) are cryptic species of the *Tetramorium caespitum* complex distinguishable using genetic (Nuclear AFLP markers and COXI analysis), morphometric characters on workers and qualitative male genital morphology (Wagner et al., 2017). *Tetramorium immigrans* is an invasive species in North America, where it was introduced in cities in the 19th century or earlier (Steiner et al., 2008) and is considered native

in Europe where its status has never been investigated. However, a previous study in the Lyon urban area showed that *T. immigrans* occurred in fragmented and warm areas and questioned its status in Europe (Gippet et al., 2017). According to Wagner et al. (2017), *T. caespitum* seems to be distributed in most regions of Europe, the Caucasus, and Anatolia.

2.1 | Microsatellite data

Cordonnier et al. (2019) collected one ant worker per colony in 1690 colonies of *Tetramorium* belonging to five species (*Tetramorium semilaeve* André, 1883, *T. forte* Forel, 1904, *T. moravicum* Kratochvíl, 1941, *T. immigrans*, and *T. caespitum*). Sampling was carried out

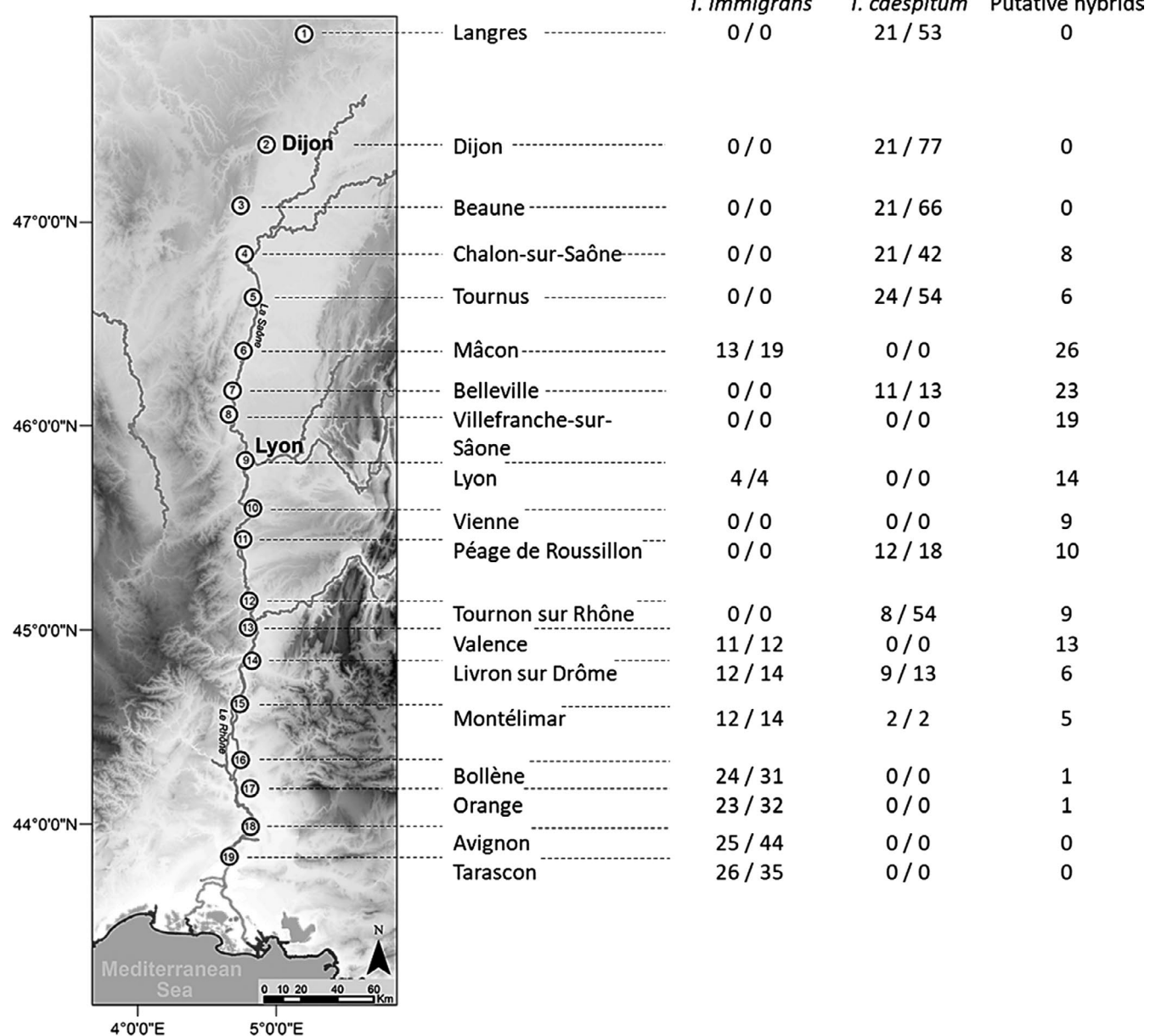


FIGURE 1 Left—Map of the 19 sampling zones. Main rivers are indicated in dark gray; altitude is indicated by grayscale (black = high altitude). Right—for each sampling zone, number of randomly chosen individuals/number of individuals assigned to *T. immigrans* and *T. caespitum* based on Q-value >0.99 in Cordonnier et al. (2019) and number of putative hybrids

along a 460 km climatic gradient located in France, east of the Saône and Rhône Rivers, extending from the city of Langres in the North (47°51'12"N, 5°20'02"E) to the city of Tarascon in the South (43°48'21"N, 4°39'37"E). Samples were collected along a predefined path in diverse environments including urban pavements, roadsides, public parks, orchards, farmlands, fields, vineyards, meadows, riverbanks and forest, in 2015 and 2016 from April to September on non-rainy days with temperatures ranging from 16 to 28°C, with a minimum distance of 200 m between two colonies. Collected ants were stored in 96% ethanol. Samples were deposited as voucher material in the collection UCBLZ, CERESE, Université de Lyon, Université Claude Bernard Lyon1.

Cordonnier et al. (2019) successfully identified 544 workers of *T. immigrans* and 698 workers of *T. caespitum* using a two-step approach combining nuclear DNA clustering (14 microsatellite markers) and species identification by mtDNA COXI sequencing. However, this sample also included 285 individuals that could not be identified because they were simultaneously associated to several species based on their genotypes, 240 of them having an intermediate genotype between *T. immigrans* and *T. caespitum* (i.e., their sum of membership coefficients for these two species was higher than 0.95). All these individuals were removed from the study by Cordonnier et al. (2019) and have therefore never been analyzed. In the present study, we selected for analyses all the 150 of the 240 individuals with admixed *T. immigrans*/*T. caespitum* genotypes, whose summed membership between these two species were >0.99, and whose genotypes were complete, without any missing allele. In addition, in order to ensure a balanced sampling design (Puechmaille, 2016), we randomly sampled 150 individuals from pure parental species (membership >0.99 in a single species) for both species, to make sure that these individuals were representative of the entire area sampled in Cordonnier et al. (2019). Our final dataset included genotypes for 14 microsatellite markers (described in Cordonnier et al., 2019) for this set of 150 *T. immigrans*, 150 *T. caespitum* and 150 putative hybrids (Figures 1 and S1). Following recommendations provided in Burgarella et al. (2009) and Vähä and Primmer (2006), we used simulated data to assess which method would provide the most reliable results in our experimental system. We used the computer program HYBRIDLAB 1.0 (Nielsen, Bach, & Kotlicki, 2006) to simulate 150 multilocus F1 hybrid genotypes between *T. caespitum* and *T. immigrans*, and 150 multilocus first-generation backcrosses (75 with each of the parental species) based on the 150 genotypes of each pure species described above. We then assembled two comparative datasets combining (a) the 300 parental genotypes and the 150 simulated F1 hybrids, and (b) the 300 parental genotypes and the 150 simulated backcrosses, respectively.

2.2 | Mitochondrial DNA data

To improve discrimination between situations with only first-generation hybrids and situations with backcrosses, a stretch of the mitochondrial cytochrome c oxidase subunit 1 gene (COXI) was sequenced in 92 individuals (11 *T. caespitum*, 44 *T. immigrans*, and

37 hybrids). COXI was amplified by PCR using specific primers developed from longer stretches of COXI from the literature (Schlick-Steiner et al., 2006; Tetra_F: TAGCATCTAATRTCTTCAYAGAGG, Tetra_R: AGTATCAGGATAATCTGAGTAYCGAC) in a 30 µl total volume of 170 µM dNTPs, 0.1 µg/µl BSA (Biolabs, B9001S), 0.16 µM of primers, 1.5 mM MgCl₂, 2 µl DNA, 1.2 U Taq Polymerase (Eurobio, GAETAQ00), and 1x PCR Buffer (Eurobio, GAETAQ00). Amplifications consisted in 5 min at 94°C, then 40 cycles (30 s at 94°C, 30 s at 48°C, and 30 s at 72°C), and 5 min at 72°C. After purification, products were sequenced (service provided by BIOFIDAL on a ABI 3730xl sequencer) and compared to known sequences from GenBank using Blast-n to identify the COXI-cluster (fragment lengths of 400–756 bp). GenBank accession numbers (MH398247–MH398302) are available in Table S1.

2.3 | Analyses

2.3.1 | Putative hybrid assignment based on genotypes

To determine the status of the 150 putative hybrids, we used assignment methods implemented in STRUCTURE v. 2.3.1 (Pritchard et al., 2000), NEWHYBRIDS (Anderson & Thompson, 2002), and Snapclust (Beugn et al., 2018) on genotypes of putative hybrids, simulated F1 and backcrosses. STRUCTURE was used to identify the ancestry composition of individuals, based on the admixture model with correlated allele frequencies, K = 2 clusters with ten iterations (K = 1–4 results in Table S2). Each run consisted in 500,000 replicates of the MCMC after a burn-in of 500,000 replicates. Clustering results were analyzed using CLUMPP v. 1.2.2 (Jakobsson & Rosenberg, 2007) to determine the proportion of individual genomes originating from each cluster (Q-values). As STRUCTURE does not allow labeling hybrids with an associated probability, we used two alternative methods to measure hybrid status. Snapclust relies on the combination of a geometric approach (i.e., it clusters individuals based on their distances in the genetic space spanned by the allelic data, without assuming a specific population genetics model; Jombart, Devillard, & Balloux, 2010) and fast likelihood optimization to more explicitly identify the hybrids between the two parental populations (Beugn et al., 2018). The results of Beugn et al. (2018) on simulated backcrossed individuals showed that the use of membership assignment probabilities corresponding to backcrosses were not accurate enough to categorize individuals unambiguously. We therefore looked for group membership probabilities for both parental species and potential hybrids using hybridization coefficients corresponding to F1 (0.5) (see Figure S2 for results based on backcrosses coefficients 0.25 and 0.75). As Snapclust does not discriminate backcrosses unambiguously, we specifically addressed the question of current introgression using NEWHYBRIDS to estimate the posterior probabilities (q) that an individual falls into five different genotype frequency classes: two parental classes (*T. caespitum* and *T. immigrans*) and three hybrid categories (F1, backcross with *T. caespitum*, and backcross with *T. immigrans*). The analysis was performed based on ten iterations carried out

using Jeffreys's prior and setting the burn-in period to 20,000, with a MCMC length of 500,000 replicates.

We used several approaches to assign the analyzed individuals to a single genetic class. First, case-specific evaluations based on comparison with simulated genotypes of known ancestry were needed, because the reliability of outputs from assignment methods depends on the type and number of markers, hybridization rate, and sampling quality. We therefore compared results obtained in the four pools of individuals (pure parental individuals, simulated backcrosses, simulated F1 hybrids, and real putative hybrids) for each three assignment methods both graphically and numerically.

We used a Q-value threshold $Tq = 0.95$, above which individuals were assigned to one genetic class, that is, pure parental, F1 hybrid, or backcross (NEWHYBRIDS, *Snapclust*), allowing comparison of these assignments with the Q-values obtained in STRUCTURE. Finally, we explored the distribution of individuals of each pool (pure parental individuals, simulated backcrosses, simulated F1 hybrids, and real putative hybrids) in six ranges of Q-value (0.5–0.6, 0.6–0.7, 0.7–0.8, 0.8–0.9, 0.9–0.95, >0.95) for the three assignment methods used here. For parental individuals, these distributions were systematically calculated based on analyses of the putative parent and hybrid data set.

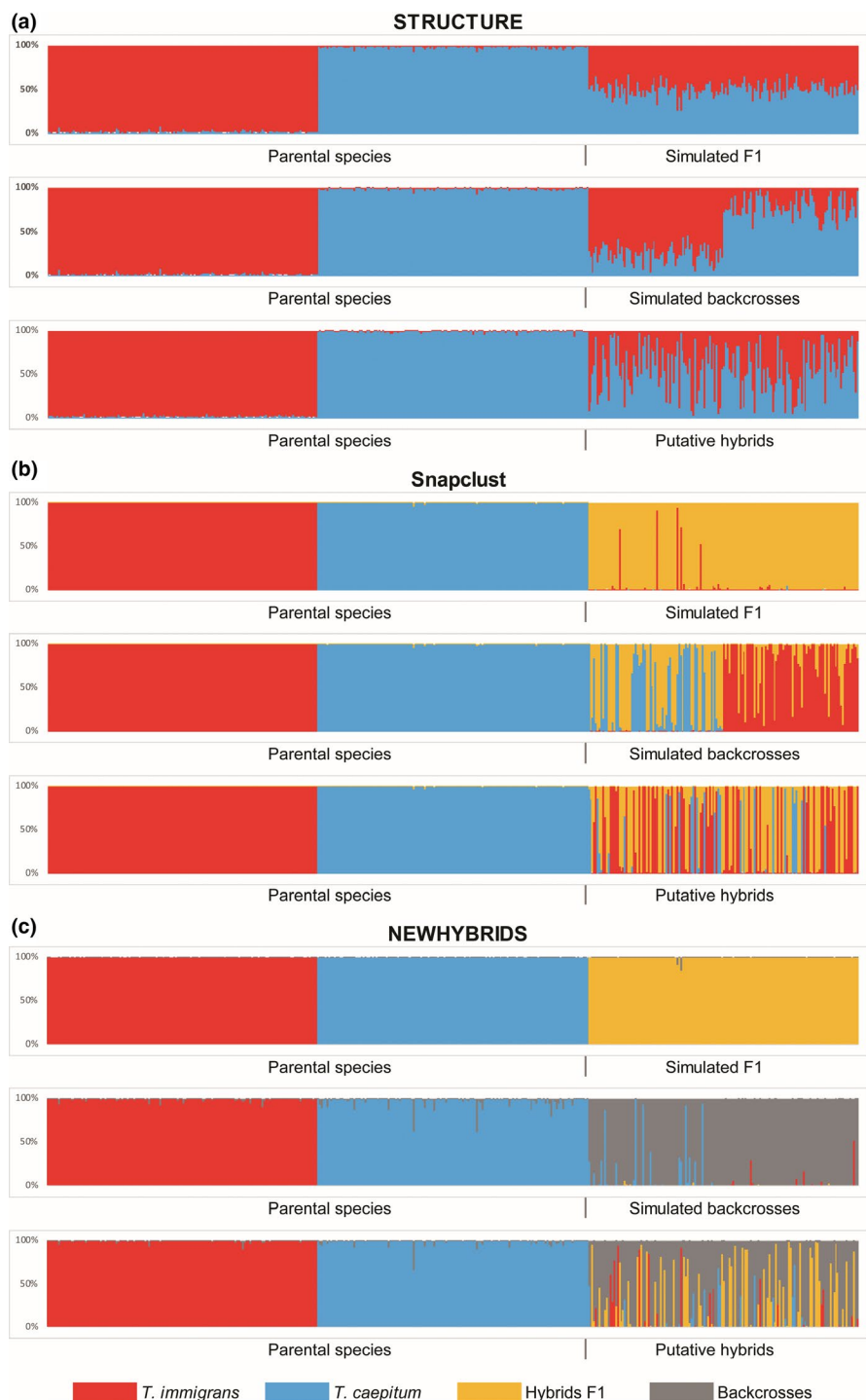


FIGURE 2 Barplots obtained for *T. caespitum*, *T. immigrans* and the three groups of hybrids (simulated F1, simulated backcrosses, and putative hybrids) and the three clustering methods (a: STRUCTURE, b: Snapclust, c: NEWHYBRIDS). Each vertical line corresponds to an individual. Individuals are always represented in the same order in all sub-figures. Colors indicate membership to each category (*T. caespitum* in red; *T. immigrans* in blue; F1 hybrids in yellow, and backcrosses in gray)

2.3.2 | Spatially explicit validation of the results

Previous studies revealed that latitudinal distributions of *T. caespitum* and *T. immigrans* are partially overlapping in the sampling area, *T. immigrans* being found more to the south than *T. caespitum*, with a sympatric zone between approximately 44.8 and 47°N (Cordonnier et al., 2019). We checked the consistency of our results in terms of spatial distribution of hybrids compared to parental species to confirm that the presence of hybrids was restricted to areas where both parental species are sympatric. For this purpose, we used latitudinal locations of hybrid individuals (including F1 and backcrosses) with congruent genotypic identification for all three methods, or with at least two congruent methods and not contradictory third (i.e., where an individual was assigned to no other class). We also used latitudinal locations of all 544 workers of *T. immigrans* and 698 workers of *T. caespitum* identified in Cordonnier et al. (2019). We then tested differences in terms of latitudinal

location between *T. immigrans*, *T. caespitum*, and interspecific hybrids to confirm that hybrids are located in intermediate latitudes compared to parental species. As latitudes are not normally distributed, we used a non-parametric Kruskal–Wallis test coupled with Mann–Whitney–Wilcoxon tests for contrasts (including a simple Bonferroni correction).

3 | RESULTS

All three assignment methods lead to very similar results whatever the pool of individuals (pure parental individuals, simulated backcrosses, simulated F1 hybrids, and real putative hybrids; Figure 2; Table S2). Graphical patterns clearly show that the set of putative hybrids neither corresponded to situations with only parental species (pure individuals) nor with only F1 hybrids, and therefore necessarily included backcrosses (Figure 2).

Q-values	Pure parents (%)	Simulated back-crosses (%)	Simulated F1 (%)	Putative hybrids (%)
>0.95	99.0	10.0	0.0	7.3
0.9–0.95	1.0	8.0	0.0	12.0
0.8–0.9	0.0	19.3	0.0	24.0
0.7–0.8	0.0	33.3	1.3	12.0
0.6–0.7	0.0	22.7	16.7	16.0
0.5–0.6	0.0	6.7	81.3	28.7

Note: For instance, 99% of the individuals initially assigned to pure species have been assigned to STRUCTURE clusters with Q-values >0.95. Classes sharing more than 50% of individuals are indicated in bold. The sum of each column is equal to 100% (corresponding to the 150 individuals belonging to this class).

TABLE 1 Distribution of individuals of each preliminary pool (pure parental individuals, simulated backcrosses, simulated F1 hybrids, and real putative hybrids) in six ranges of Q-value (0.5–0.6, 0.6–0.7, 0.7–0.8, 0.8–0.9, 0.9–0.95, >0.95) resulting from STRUCTURE assignment

	Pure parents (%)	Simulated back-crosses (%)	Simulated F1 (%)	Putative hybrids (%)
Parental species membership probabilities				
>0.95	100.0	36.7	0.0	38.7
0.9–0.95	0.0	6.7	1.3	4.7
0.8–0.9	0.0	7.3	0.0	7.3
0.7–0.8	0.0	7.3	0.7	2.0
0.6–0.7	0.0	4.7	0.7	4.0
0.5–0.6	0.0	1.3	0.7	3.3
F1 hybrids membership probabilities				
>0.95	0.0	19.3	94.7	32.7
0.9–0.95	0.0	6.0	2.0	3.3
0.8–0.9	0.0	6.7	0.0	0.7
0.7–0.8	0.0	3.3	0.0	3.3
0.6–0.7	0.0	0.0	0.0	0.0
0.5–0.6	0.0	0.7	0.0	0.0

Note: For instance, 100% of the individuals initially assigned to pure species have been assigned to Snapclust Parental species clusters with Q-values >0.95. Classes sharing more than 50% of individuals are indicated in bold. The sum of each column is equal to 100% (corresponding to the 150 individuals belonging to this class).

TABLE 2 Distribution of individuals of each preliminary pool (pure parental individuals, simulated backcrosses, simulated F1 hybrids, and real putative hybrids) in six ranges of membership probabilities (0.5–0.6, 0.6–0.7, 0.7–0.8, 0.8–0.9, 0.9–0.95, >0.95) resulting from Snapclust assignment

TABLE 3 Distribution of individuals of each preliminary pool (pure parental individuals, simulated backcrosses, simulated F1 hybrids, and real putative hybrids) in six ranges of membership probabilities (0.5–0.6, 0.6–0.7, 0.7–0.8, 0.8–0.9, 0.9–0.95, >0.95) resulting from NEWHYBRIDS assignment

		Pure parents (%)	Simulated back-crosses (%)	Simulated F1 (%)	Putative hybrids (%)
Parental species membership probabilities					
>0.95	95.7	0.3	0.0	0.0	0.0
0.9–0.95	3.7	1.0	0.0	0.0	0.7
0.8–0.9	0.3	0.3	0.0	0.0	0.7
0.7–0.8	0.0	0.0	0.0	0.0	1.3
0.6–0.7	0.3	0.0	0.0	0.0	0.7
0.5–0.6	0.0	0.3	0.0	0.0	0.7
Backcrosses membership probabilities					
>0.95	0.0	83.3	0.0	0.0	40.7
0.9–0.95	0.0	2.0	0.0	0.0	4.7
0.8–0.9	0.0	3.3	0.0	0.0	4.7
0.7–0.8	0.0	4.7	0.0	0.0	5.3
0.6–0.7	0.0	2.0	0.0	0.0	5.3
0.5–0.6	0.0	0.7	0.0	0.0	5.3
F1 hybrids membership probabilities					
>0.95	0.0	0.0	98.7	0.0	5.3
0.9–0.95	0.0	0.0	0.7	0.0	3.3
0.8–0.9	0.0	0.0	0.7	0.0	6.7
0.7–0.8	0.0	0.0	0.0	0.0	4.0
0.6–0.7	0.0	0.0	0.0	0.0	2.7
0.5–0.6	0.0	0.0	0.0	0.0	4.0

Note: For instance, 95.7% of the individuals initially assigned to pure species have been assigned to NEWHYBRIDS Parental species clusters with Q-values >0.95. Classes sharing more than 50% of individuals are indicated in bold. The sum of each column is equal to 100% (corresponding to the 150 individuals belonging to this class).

Distributions of individual Q-values of each pool (pure parental individuals, simulated backcrosses, simulated F1 hybrids, and real putative hybrids) confirm that putative hybrids were the product of F1 crosses but also backcrosses with parental species (Tables 1–3).

Among the 150 potential hybrids tested, STRUCTURE identified 139 individuals as hybrids based on Q-value between 0.05 and 0.95. Three individuals were classified as *T. caespitum* and eight as *T. immigrans*. NEWHYBRIDS identified 61 backcross individuals, 8 F1 hybrids, and 81 unclassifiable individuals based on 0.95 threshold value. Finally, using Snapclust, 58 individuals were considered pure parents (49 *T. immigrans* and nine *T. caespitum*), 49 F1 hybrids, and 43 were unclassifiable, corresponding to putative backcrosses. Table 4 shows the results based on the different assignment methods. The assignment of individuals based on the threshold Tq = 0.95 in NEWHYBRIDS and Snapclust did not always correspond to assignments obtained using STRUCTURE.

Snapclust favored parental species detection compared to other assignment methods (Tables 2 and 4), whereas NEWHYBRIDS detected no parental species in the putative hybrid pool (Table 3). Threshold Q-value of 0.95 in STRUCTURE appeared accurate to categorize an individual as pure species and strictly avoided inclusion of F1 hybrid individuals leading to misidentification of parental species (Table 4).

TABLE 4 Range of Q-values obtained for the empirical (not simulated) data as a result of Bayesian clustering computed in STRUCTURE for each category of individuals defined by NEWHYBRIDS and Snapclust analyses (threshold value Tq > 0.95)

	min STRUCTURE Q-value	max STRUCTURE Q-value
Backcross [NEWHYBRIDS]	0.057	0.943
F1 Hybrids [NEWHYBRIDS]	0.393	0.607
Parental species [NEWHYBRIDS]	0.935	0.994
F1 Hybrids [Snapclust]	0.282	0.718
Parental species [Snapclust]	0.721	0.994

Considering that an individual belongs to a pure species when Q-value is above 0.95 also limits the risks of assigning a potential backcrossed individual to parental species with a 10% error threshold (Table 1).

Regarding the distribution of hybrids relative to the parental species, latitudinal locations of individuals assigned to hybrids categories were intermediate between *T. immigrans* and *T. caespitum* (Figure 3).

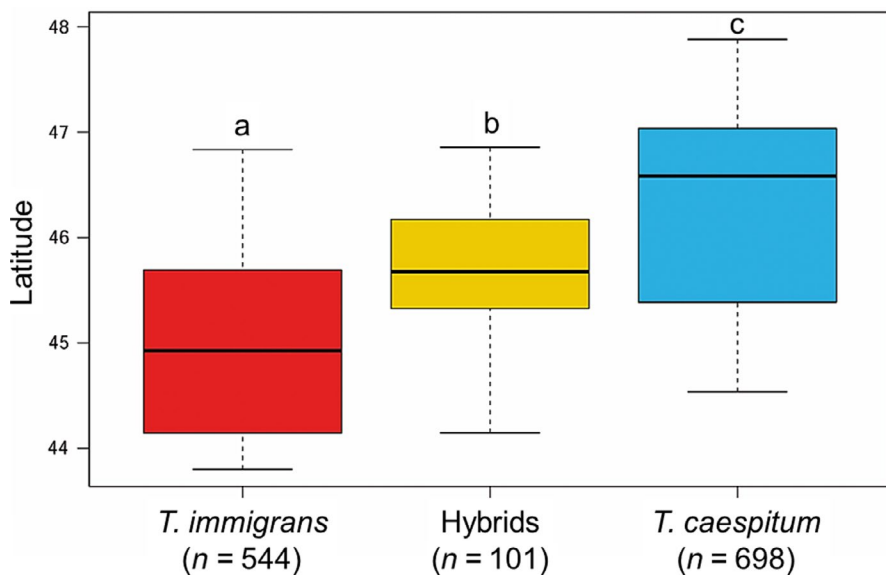


FIGURE 3 Latitudinal distributions of the individuals confirmed as hybrids and as pure parental species (Kruskal–Wallis chi-squared = 479.74, $df = 2$, p -value $<2.2 \times 10^{-16}$). Thick black horizontal line: median value; box ends: first and third quartiles; whiskers: min and max values. Letters a, b, c indicate the results of the non-parametric Mann–Whitney–Wilcoxon tests (a–b: $W = 41,030$, p -value = 3.2×10^{-15} ; a–c: $W = 55,640$, p -value $<2.2 \times 10^{-16}$; b–c: $W = 20,032$, p -value = 2.2×10^{-12})

Finally, regarding the mitochondrial DNA data, nine out of the 13 F1 hybrids defined by their genotypes (i.e., based on congruent genotypic identification for all three methods, or with at least two congruent methods and no contradictory third) had haplotypes associated with *T. immigrans*, 12 of the 15 *T. immigrans* backcrosses had a *T. immigrans* haplotype and 8 of the 9 *T. caespitum* backcrosses had a *T. caespitum* haplotype (Figure S3). Discordance frequency between nuclear assignment and mitochondrial haplotypes was similar in each parental species (respectively three out of 44 genotyped *T. immigrans* with Structure Q-values = 0.996, 0.994, and 0.996 and coming from sampling zones of Tarascon, Vienne and Bollène and one out of 11 genotyped *T. caespitum* with Structure Q-values = 0.986 and coming from the sampling zone of Vienne), which suggests a bidirectional (in both parental species) and symmetric (with the same prevalence) mitochondrial introgression.

4 | DISCUSSION

The present study proves the existence of hybridization processes between *Tetramorium immigrans* and *T. caespitum*. Results clearly demonstrate the existence of backcrossing between hybrids and parental species based on three methods and comparisons with simulated data. Results are spatially consistent, with hybrids located at latitudes where parental species are sympatric. In addition, mitochondrial-nuclear discordances suggest bidirectional and symmetric introgression between these species.

The 150 sampled individuals not fully assigned to *T. immigrans* or *T. caespitum* in Cordonnier et al. (2019) (Q -values <0.95) thus appear to result from hybridization between these two species. The same detection methods based on a Q -value threshold have been already described for other taxa, for example, between populations of wild and domestic cats in Italy (Randi, Pierpaoli, Beaumont, Ragni, & Sforzi, 2001), between two oak species (*Quercus suber* and *Q. ilex*; Burgarella et al., 2009), or between invasive sika and native red

deer (*Cervus Nippon* and *C. elaphus*; Senn & Pemberton, 2009), as well as in ants, for example, between *Formica selysi* and *F. cinerea* (Purcell et al., 2016). Ito, Langenhorst, Ogden, and Inoue-Murayama (2015) considered that a high qi threshold value (>0.95) confidently identifies pure individuals and allows the exclusion of potential hybrids. However, the reliability of assignment methods depends on the type and number of markers, the hybridization rate, and the quality of the sampling (e.g., Väähä & Primmer, 2006). Therefore, the use of a threshold of 0.95 to differentiate hybrids from parental species should be verified in each studied system, through a robust approach based on the multiplicity of methods and confirmation through simulations. Here, we confirm that the qi threshold value of 0.95 proposed in Cordonnier et al. (2019) to consider an individual as belonging to a pure species ensures that no F1 hybrid individuals are erroneously assigned to parental species. All three methods were congruent in recovering parental populations and discriminating individuals from both F1 hybrid and backcross classes. However, *Snapclust* tended to over-detect parental species compared to other assignment methods, whereas NEWHYBRIDS detected no parental species in the putative hybrid pool and was the most accurate at properly assigning the simulated F1 hybrids and backcrossed individuals. Together, these findings clearly support the use of hyper variable microsatellite markers to identify F1 and backcrossed hybrids, and the use of the combination of nuclear and mitochondrial data to confirm the existence of mitochondrial introgression. In our view, such introgression rules out all risks of misinterpretation concerning hybrid status that may exist due to limitations of assignment-based methods when dealing with admixture data (e.g., Lawson, Dorp, & Falush, 2018). Hybridization is sometimes incompatible with the use of DNA barcodes for species delimitation (e.g., Dupont, Porco, Symondson, & Roy, 2016), more especially in haplodiploid systems (Patten et al., 2015). The mito-nuclear discordances found in our study make barcode species identification within the *Tetramorium caespitum* complex questionable. Finally, it could be interesting to investigate the possibility and usefulness of morphometrics for these

species to detect hybrids in the future. Indeed, an in-depth morphometric study may be relevant and less expensive in a complex where integrative taxonomy combining both molecular and morphometric approaches have solved major taxonomic problems (Wagner et al., 2017).

The large set of putative hybrids tested here included numerous backcrosses (more than 40% according to NEWHYBRIDS), revealing the first clues of interspecific reproductive events leading to fertile offspring, and older cryptic hybrids could be present in the dataset and not detected here. The occurrence of backcrossed individuals indicates that hybrid queens or males are fertile, which is confirmed by the presence of mitochondrial haplotypes of one species within another. The discovery of fertile hybrids is unusual in ants (Purcell et al., 2016; Feldhaar et al., 2008; but see Seifert, Kulmuni, & Pamilo, 2010), and is particularly interesting as the numerous backcrosses compared to F1 hybrids may reveal a high fitness of hybrids, or at least a weak selection against hybrids. In such situations, hybridization sometimes results in the extirpation of one of the parental species or in the replacement of species pairs by hybrid swarms (Gilman & Behm, 2011). Interspecific hybridization may allow adaptive combinations to evolve at a higher rate (Mallet, 2005), therefore increasing the fitness of hybrids (Twyford & Ennos, 2012). Moreover, hybridization is a powerful engine for speciation, especially when hybrid lineages are ecologically or spatially divergent from the parent species (Twyford & Ennos, 2012). Previous studies about hybrid zones in ants have already provided insights into speciation. For example, Cahan and Vinson (2003) showed that *Solenopsis xyloni* evolved a social hybridogenesis in the hybrid zone with *S. geminata*, leading to obligate hybridization for worker production, but preventing hybrids from being represented in the reproductive caste (which is not the case here as the existence of backcrossed individuals show that hybrids can develop into fertile, reproductive individuals). Purcell et al. (2016) worked on the hybrid zone between *Formica selysi* and *F. cinerea* and showed an asymmetric distribution of hybrids skewed toward *F. cinerea*, suggesting a pattern of unidirectional nuclear gene flow from *F. selysi* into *F. cinerea*. The hybrid zone detected in the present study should therefore be studied much deeper in the future as it could provide a suitable system to investigate speciation in social insects.

Hybridization must be considered not only in its genetic but also in its ecological context. Studying the biological mechanisms facilitating interspecific mating between *T. immigrans* and *T. caespitum* should improve our understanding of hybridization processes between them. Wagner et al. (2017) already suggested that hybridization between these species might be facilitated by similar male genital morphology, overlapping phenology, and frequent sympatric occurrence. Since there are no anatomical barriers to mating between these species, the production of hybrid offspring might result from a low discrimination ability of the heterospecific partners. Studying whether hybridization is favored preferentially in males or females is also necessary, as Kulmuni and Pamilo (2014) showed that in two hybridized *Formica* species introgression is favored in diploid females but selected against in haploid males. It will be therefore

necessary to measure whether hybrid queens or hybrid males (occurring in the next generation, from an introgressed mother) are equally produced in the *T. caespitum/T. immigrans* hybrid system and to investigate if both sexes can produce viable offspring.

Finally, large-scale processes involved in the setting up of the hybrid zone described here should be explored. Increases in rates of hybridization and introgression are often attributed to translocations of organisms by humans (Allendorf et al., 2001). Across ant taxa, Feldhaar et al. (2008) predicted that detailed research should reveal numerous additional cases of hybridization, in particular in those ant faunas that are characterized by the recent introduction of multiple invasive species. In addition, hybridization may play a significant role for introduced species to become invasive (Allendorf & Luikart, 2007; Ellstrand & Schierenbeck, 2000; Hall, 2016), for example, allowing genetically admixed individuals to invade novel niches unoccupied by any of their parent species (Roy, Lucek, Walter, & Seehausen, 2015). Habitat disturbance is also considered responsible for the increase in hybridization between species in recent years. Indeed, hybridization between naturally co-occurring species that normally do not interbreed is being documented following anthropogenic habitat modifications for an increasing number of taxa (Allendorf et al., 2001; Grabenstein & Taylor, 2018). Finally, climate changes also promote hybridization or introgression. In response to climate changes, species change their distributions, leading to new contact zones between previously isolated taxa (Brennan et al., 2015).

Given latitude overlap between the distribution of *T. caespitum* and *T. immigrans* (Cordonnier et al., 2019), the potential role of urbanization-induced disturbance in habitats on the presence of *T. immigrans* (Cordonnier et al., ongoing work; Gippet et al., 2017; Wagner et al., 2017), the fact that *T. immigrans* is invasive in North America (Steiner et al., 2006, 2008) and has a questioned status in France (Gippet et al., 2017), but also in other parts of Europe (Borowiec & Salata, 2018; Wagner, 2011), the causes and consequences of hybridization will deserve further investigation focused on the hybridization zone delineated in the present study.

ACKNOWLEDGEMENTS

This study was funded by the Conseil Départemental de l'Isère. It was also supported by the French National Research Agency (ANR) through the LABEX IMU (ANR-10-LABX-0088) of Université de Lyon, within the program "Investissements d'Avenir" (ANR-11-IDEX-0007).

ORCID

Marion Cordonnier  <https://orcid.org/0000-0003-3431-1344>

REFERENCES

- Allendorf, F. W., Leary, R. F., Spruell, P., & Wenburg, J. K. (2001). The problems with hybrids: Setting conservation guidelines. *Trends*

- in *Ecology & Evolution*, 16(11), 613–622. [https://doi.org/10.1016/S0169-5347\(01\)02290-X](https://doi.org/10.1016/S0169-5347(01)02290-X)
- Allendorf, F. W., & Luikart, G. (2007). Conservation and the genetics of populations. *Mammalia*, 2007(2007), 189–197.
- Allendorf, F. W., & Luikart, G. (2009). *Conservation and the genetics of populations*. London: John Wiley & Sons.
- Anderson, E. (1953). Introgressive hybridization. *Biological Reviews*, 28(3), 280–307. <https://doi.org/10.1111/j.1469-185X.1953.tb01379.x>
- Anderson, E. C., & Thompson, E. A. (2002). A model-based method for identifying species hybrids using multilocus genetic data. *Genetics*, 160(3), 1217–1229.
- Arnold, M. L. (1992). Natural hybridization as an evolutionary process. *Annual Review of Ecology and Systematics*, 23(1), 237–261. <https://doi.org/10.1146/annurev.es.23.110192.001321>
- Arnold, M. L. (2006). *Evolution through genetic exchange*. Oxford: Oxford University Press.
- Arnold, M. L., & Kunte, K. (2017). Adaptive genetic exchange: A tangled history of admixture and evolutionary innovation. *Trends in Ecology & Evolution*, 32(8), 601–611. <https://doi.org/10.1016/j.tree.2017.05.007>
- Barton, N. H., & Hewitt, G. M. (1989). Adaptation, speciation and hybrid zones. *Nature*, 341(6242), 497.
- Beugn, M. P., Gayet, T., Pontier, D., Devillard, S., & Jombart, T. (2018). A fast likelihood solution to the genetic clustering problem. *Methods in Ecology and Evolution*, 9(4), 1006–1016. <https://doi.org/10.1111/2041-210X.12968>
- Bohling, J. H., Adams, J. R., & Waits, L. P. (2013). Evaluating the ability of Bayesian clustering methods to detect hybridization and introgression using an empirical red wolf data set. *Molecular Ecology*, 22(1), 74–86. <https://doi.org/10.1111/mec.12109>
- Borowiec, L., & Salata, S. (2018). *Tetramorium immigrans* SANTSCHI, 1927 (Hymenoptera: Formicidae) nowy gatunek potencjalnie invazyjnej mrówki w Polsce. *Acta Entomologica Silesiana*, 26, 1–5.
- Brennan, A. C., Woodward, G., Seehausen, O., Muñoz-Fuentes, V., Moritz, C., Guelmami, A., ... Edelaar, P. (2015). Hybridization due to changing species distributions: Adding problems or solutions to conservation of biodiversity during global change? *Evolutionary Ecology Research*, 16(6), 475–491.
- Burgarella, C., Lorenzo, Z., Jabbour-Zahab, R., Lumaret, R., Guichoux, E., Petit, R. J., ... Gil, L. (2009). Detection of hybrids in nature: Application to oaks (*Quercus suber* and *Q. ilex*). *Heredity*, 102(5), 442–452. <https://doi.org/10.1038/hdy.2009.8>
- Butler, I. A., Peters, M. K., & Kronauer, D. J. C. (2018). Low levels of hybridization in two species of African driver ants. *Journal of Evolutionary Biology*, 31(4), 556–571. <https://doi.org/10.1111/jeb.13245>
- Cabria, M. T., Michaux, J. R., Gómez-Moliner, B. J., Skumatov, D., Maran, T., Fournier, P., ... Zardoya, R. (2011). Bayesian analysis of hybridization and introgression between the endangered european mink (*Mustela lutreola*) and the polecat (*Mustela putorius*). *Molecular Ecology*, 20(6), 1176–1190. <https://doi.org/10.1111/j.1365-294X.2010.04988.x>
- Cahan, S. H., & Vinson, S. B. (2003). Reproductive division of labor between hybrid and nonhybrid offspring in a fire ant hybrid zone. *Evolution*, 57(7), 1562–1570. <https://doi.org/10.1111/j.0014-3820.2003.tb00364.x>
- Corander, J., & Marttinen, P. (2006). Bayesian identification of admixture events using multilocus molecular markers. *Molecular Ecology*, 15(10), 2833–2843. <https://doi.org/10.1111/j.1365-294X.2006.02994.x>
- Cordonnier, M., Bellec, A., Dumet, A., Escarguel, G., & Kaufmann, B. (2019). Range limits in sympatric cryptic species: A case study in *Tetramorium pavement* ants (Hymenoptera: Formicidae) across a biogeographical boundary. *Insect Conservation and Diversity*, 12(2), 109–120. <https://doi.org/10.1111/icad.12316>
- Currat, M., Ruedi, M., Petit, R. J., & Excoffier, L. (2008). The hidden side of invasions: Massive introgression by local genes. *Evolution: International Journal of Organic Evolution*, 62(8), 1908–1920.
- Darras, H., & Aron, S. (2015). Introgression of mitochondrial DNA among lineages in a hybridogenetic ant. *Biology Letters*, 11(2), 20140971. <https://doi.org/10.1098/rsbl.2014.0971>
- Dejaco, T., Gassner, M., Arthofer, W., Schlick-Steiner, B. C., & Steiner, F. M. (2016). Taxonomist's nightmare... evolutionist's delight: An integrative approach resolves species limits in jumping bristletails despite widespread hybridization and parthenogenesis. *Systematic Biology*, 65(6), 947–974. <https://doi.org/10.1093/sysbio/syw003>
- Dupont, L., Porco, D., Symondson, W. O. C., & Roy, V. (2016). Hybridization relics complicate barcode-based identification of species in earthworms. *Molecular Ecology Resources*, 16(4), 883–894. <https://doi.org/10.1111/1755-0998.12517>
- Ellstrand, N. C., & Schierenbeck, K. A. (2000). Hybridization as a stimulus for the evolution of invasiveness in plants? *Proceedings of the National Academy of Sciences*, 97(13), 7043–7050. <https://doi.org/10.1073/pnas.97.13.7043>
- Endler, J. A. (1977). *Geographic variation, speciation, and clines* (No. 10). Princeton: Princeton University Press.
- Excoffier, L., Foll, M., & Petit, R. J. (2009). Genetic consequences of range expansions. *Annual Review of Ecology, Evolution, and Systematics*, 40, 481–501. <https://doi.org/10.1146/annurev.ecolsys.39.110707.173414>
- Falush, D., Stephens, M., & Pritchard, J. K. (2003). Inference of population structure using multilocus genotype data: Linked loci and correlated allele frequencies. *Genetics*, 164(4), 1567–1587.
- Feldhaar, H., Foitzik, S., & Heinze, J. (2008). Lifelong commitment to the wrong partner: Hybridization in ants. *Philosophical Transactions of the Royal Society of London B: Biological Sciences*, 363(1505), 2891–2899.
- Gilman, R. T., & Behm, J. E. (2011). Hybridization, species collapse, and species reemergence after disturbance to premating mechanisms of reproductive isolation. *Evolution: International Journal of Organic Evolution*, 65(9), 2592–2605. <https://doi.org/10.1111/j.1558-5646.2011.01320.x>
- Gippert, J. M., Mondy, N., Diallo-Dudek, J., Bellec, A., Dumet, A., Mistler, L., & Kaufmann, B. (2017). I'm not like everybody else: Urbanization factors shaping spatial distribution of native and invasive ants are species-specific. *Urban Ecosystems*, 20(1), 157–169. <https://doi.org/10.1007/s11252-016-0576-7>
- Grabenstein, K. C., & Taylor, S. A. (2018). Breaking barriers: Causes, consequences, and experimental utility of human-mediated hybridization. *Trends in Ecology & Evolution*, 33(3), 198–212. <https://doi.org/10.1016/j.tree.2017.12.008>
- Hall, R. J. (2016). Hybridization helps colonizers become conquerors. *Proceedings of the National Academy of Sciences*, 113(36), 9963–9964. <https://doi.org/10.1073/pnas.1611222113>
- Harrison, R. G. (1990). Hybrid zones: Windows on evolutionary process. *Oxford Surveys in Evolutionary Biology*, 7, 69–128.
- Ito, H., Langenhorst, T., Ogden, R., & Inoue-Murayama, M. (2015). Population genetic diversity and hybrid detection in captive zebras. *Scientific Reports*, 5, 13171. <https://doi.org/10.1038/srep13171>
- Jakobsson, M., & Rosenberg, N. A. (2007). CLUMPP: A cluster matching and permutation program for dealing with label switching and multimodality in analysis of population structure. *Bioinformatics*, 23(14), 1801–1806. <https://doi.org/10.1093/bioinformatics/btm233>
- Jombart, T., Devillard, S., & Balloux, F. (2010). Discriminant analysis of principal components: A new method for the analysis of genetically structured populations. *BMC Genetics*, 11(1), 94. <https://doi.org/10.1186/1471-2156-11-94>
- Kulmuni, J., & Pamilo, P. (2014). Introgression in hybrid ants is favored in females but selected against in males. *Proceedings of the National Academy of Sciences*, 111(35), 12805–12810. <https://doi.org/10.1073/pnas.1323045111>

- Kulmuni, J., Seifert, B., & Pamilo, P. (2010). Segregation distortion causes large-scale differences between male and female genomes in hybrid ants. *Proceedings of the National Academy of Sciences*, 107(16), 7371–7376. <https://doi.org/10.1073/pnas.0912409107>
- Lawson, D. J., Van Dorp, L., & Falush, D. (2018). A tutorial on how not to over-interpret STRUCTURE and ADMIXTURE bar plots. *Nature Communications*, 9(1), 3258–4000. <https://doi.org/10.1038/s41467-018-05257-7>
- Mallet, J. (2005). Hybridization as an invasion of the genome. *Trends in Ecology & Evolution*, 20(5), 229–237. <https://doi.org/10.1016/j.tree.2005.02.010>
- Mallet, J. (2007). Hybrid speciation. *Nature*, 446(7133), 279.
- Moore, W. S. (1977). An evaluation of narrow hybrid zones in vertebrates. *The Quarterly Review of Biology*, 52(3), 263–277. <https://doi.org/10.1086/409995>
- Nielsen, E. E., Bach, L. A., & Kotlicki, P. (2006). HYBRIDLAB (version 1.0): A program for generating simulated hybrids from population samples. *Molecular Ecology Notes*, 6(4), 971–973.
- Patten, M. M., Carioscia, S. A., & Linnen, C. R. (2015). Biased introgression of mitochondrial and nuclear genes: A comparison of diploid and haplodiploid systems. *Molecular Ecology*, 24(20), 5200–5210. <https://doi.org/10.1111/mec.13318>
- Pritchard, J. K., Stephens, M., Rosenberg, N. A., & Donnelly, P. (2000). Association mapping in structured populations. *The American Journal of Human Genetics*, 67(1), 170–181. <https://doi.org/10.1086/302959>
- Puechmaille, S. J. (2016). The program structure does not reliably recover the correct population structure when sampling is uneven: Subsampling and new estimators alleviate the problem. *Molecular Ecology Resources*, 16(3), 608–627.
- Purcell, J., Zahnd, S., Athanasiades, A., Türler, R., Chapuisat, M., & Brelsford, A. (2016). Ants exhibit asymmetric hybridization in a mosaic hybrid zone. *Molecular Ecology*, 25(19), 4866–4874. <https://doi.org/10.1111/mec.13799>
- Randi, E. (2008). Detecting hybridization between wild species and their domesticated relatives. *Molecular Ecology*, 17(1), 285–293. <https://doi.org/10.1111/j.1365-294X.2007.03417.x>
- Randi, E., Pierpaoli, M., Beaumont, M., Ragni, B., & Sforzi, A. (2001). Genetic identification of wild and domestic cats (*Felis silvestris*) and their hybrids using Bayesian clustering methods. *Molecular Biology and Evolution*, 18(9), 1679–1693.
- Roy, D., Lucek, K., Walter, R. P., & Seehausen, O. (2015). Hybrid 'super-swarm' leads to rapid divergence and establishment of populations during a biological invasion. *Molecular Ecology*, 24(21), 5394–5411.
- Sanz, N., Araguas, R. M., Fernández, R., Vera, M., & García-Marín, J. L. (2009). Efficiency of markers and methods for detecting hybrids and introgression in stocked populations. *Conservation Genetics*, 10(1), 225–236. <https://doi.org/10.1007/s10592-008-9550-0>
- Schlick-Steiner, B. C., Steiner, F. M., Moder, K., Seifert, B., Sanetra, M., Dyreson, E., ... Christian, E. (2006). A multidisciplinary approach reveals cryptic diversity in Western Palearctic *Tetramorium* ants (Hymenoptera: Formicidae). *Molecular Phylogenetics and Evolution*, 40(1), 259–273. <https://doi.org/10.1016/j.ympev.2006.03.005>
- Schumer, M., Rosenthal, G. G., & Andolfatto, P. (2014). How common is homoploid hybrid speciation? *Evolution*, 68(6), 1553–1560. <https://doi.org/10.1111/evo.12399>
- Schumer, M., Xu, C., Powell, D. L., Durvasula, A., Skov, L., Holland, C., ... Przeworski, M. (2018). Natural selection interacts with recombination to shape the evolution of hybrid genomes. *Science*, 360(6389), 656–660.
- Seifert, B., Kulmuni, J., & Pamilo, P. (2010). Independent hybrid populations of *Formica polyctena* X *rufa* wood ants (Hymenoptera: Formicidae) abound under conditions of forest fragmentation. *Evolutionary Ecology*, 24(5), 1219–1237. <https://doi.org/10.1007/s10682-010-9371-8>
- Senn, H. V., & Pemberton, J. M. (2009). Variable extent of hybridization between invasive sika (*Cervus nippon*) and native red deer (*C. elaphus*) in a small geographical area. *Molecular Ecology*, 18(5), 862–876.
- Steiner, F. M., Schlick-Steiner, B. C., Trager, J. C., Moder, K., Sanetra, M., Christian, E., & Stauffer, C. (2006). *Tetramorium tsushima*e, a new invasive ant in North America. *Biological Invasions*, 8(2), 117–123. <https://doi.org/10.1007/s10530-004-1249-7>
- Steiner, F. M., Schlick-Steiner, B. C., VanDerWal, J., Reuther, K. D., Christian, E., Stauffer, C., ... Crozier, R. H. (2008). Combined modeling of distribution and niche in invasion biology: A case study of two invasive *Tetramorium* ant species. *Diversity and Distributions*, 14(3), 538–545. <https://doi.org/10.1111/j.1472-4642.2008.00472.x>
- Steyer, K., Tiesmeyer, A., Muñoz-Fuentes, V., & Nowak, C. (2018). Low rates of hybridization between European wildcats and domestic cats in a human-dominated landscape. *Ecology and Evolution*, 8(4), 2290–2304. <https://doi.org/10.1002/ece3.3650>
- Taylor, S. A., Larson, E. L., & Harrison, R. G. (2015). Hybrid zones: Windows on climate change. *Trends in Ecology & Evolution*, 30(7), 398–406. <https://doi.org/10.1016/j.tree.2015.04.010>
- Toews, D. P., & Brelsford, A. (2012). The biogeography of mitochondrial and nuclear discordance in animals. *Molecular Ecology*, 21(16), 3907–3930. <https://doi.org/10.1111/j.1365-294X.2012.05664.x>
- Twyford, A. D., & Ennos, R. A. (2012). Next-generation hybridization and introgression. *Heredity*, 108(3), 179–189. <https://doi.org/10.1038/hdy.2011.68>
- Vähä, J. P., & Primmer, C. R. (2006). Efficiency of model-based Bayesian methods for detecting hybrid individuals under different hybridization scenarios and with different numbers of loci. *Molecular Ecology*, 15(1), 63–72. <https://doi.org/10.1111/j.1365-294X.2005.02773.x>
- Wagner, H. C. (2011). Tag der Artenvielfalt – Die Ameisen (Hymenoptera: Formicidae) im Botanischen Garten Graz. – Mitteilungen des naturwissenschaftlichen Vereines für Steiermark, 141, 235–240.
- Wagner, H. C., Arthofer, W., Seifert, B., Muster, C., Steiner, F. M., & Schlick-Steiner, B. C. (2017). Light at the end of the tunnel: Integrative taxonomy delimits cryptic species in the *Tetramorium caespitum* complex (Hymenoptera: Formicidae). *Myrmecological News*, 25, 95–129.

SUPPORTING INFORMATION

Additional supporting information may be found online in the Supporting Information section at the end of the article.

How to cite this article: Cordonnier M, Gayet T, Escarguel G, Kaufmann B. From hybridization to introgression between two closely related sympatric ant species. *J Zool Syst Evol Res*. 2019;00:1–11. <https://doi.org/10.1111/jzs.12297>

Supporting information

From hybridization to introgression between two closely related sympatric ant species

Marion Cordonnier, Thibault Gayet, Gilles Escarguel, Bernard Kaufmann

Figure S1. First and second axes of a PCA (implemented in R package ADEGENET) based on genotypes from the real data: 150 *Tetramorium immigrans* in red, 150 *T. caespitum* in blue, 150 putative hybrids in black. Percentages of explained variability: 2.85% (axis 1), 0.939 % (axis 2).

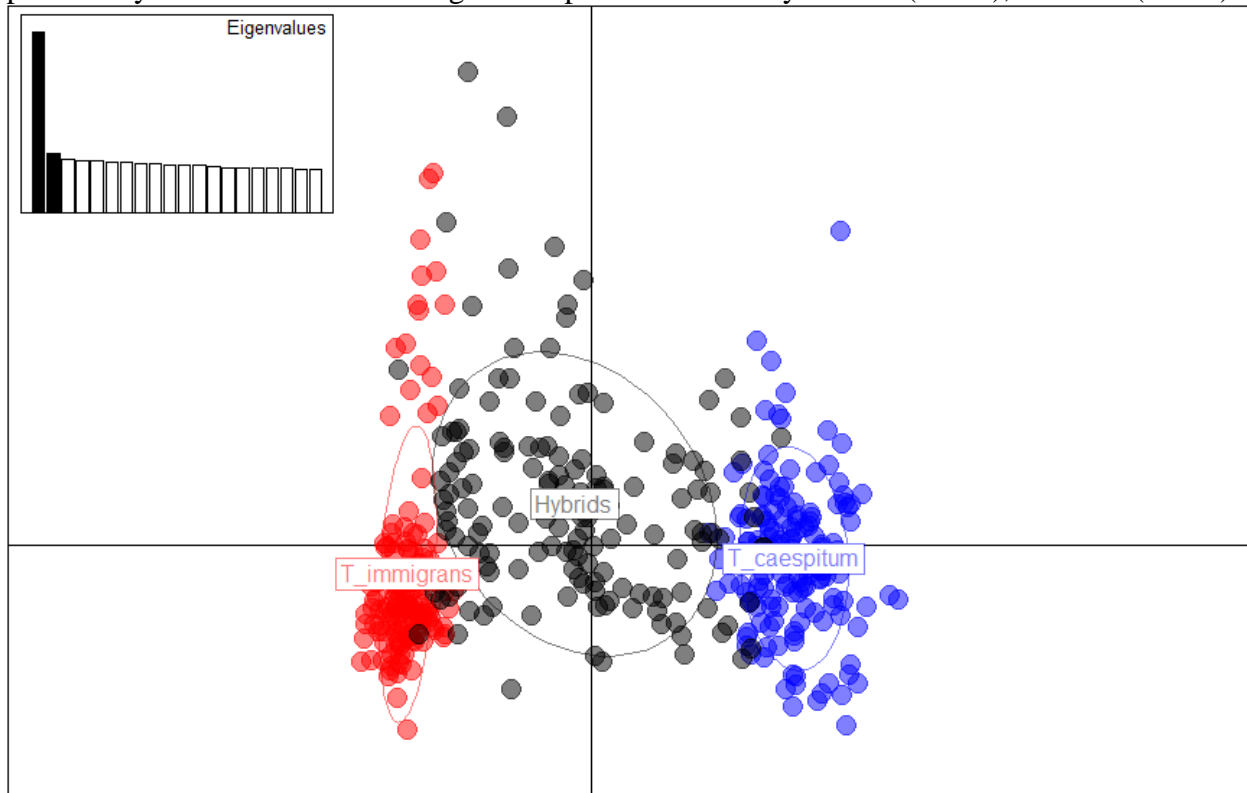


Figure S2. Barplots obtained from *Snapclust* with hybrid coefficients 0.25 and 0.5 (A: Parental species + simulated F1; B: Parental species + simulated backcrosses; C: parental species + putative hybrids). Each vertical line corresponds to an individual. Colors indicate membership to each category (*T. caespitum* in red, *T. immigrans* in blue, F1 hybrids in yellow, and backcrosses in grey).

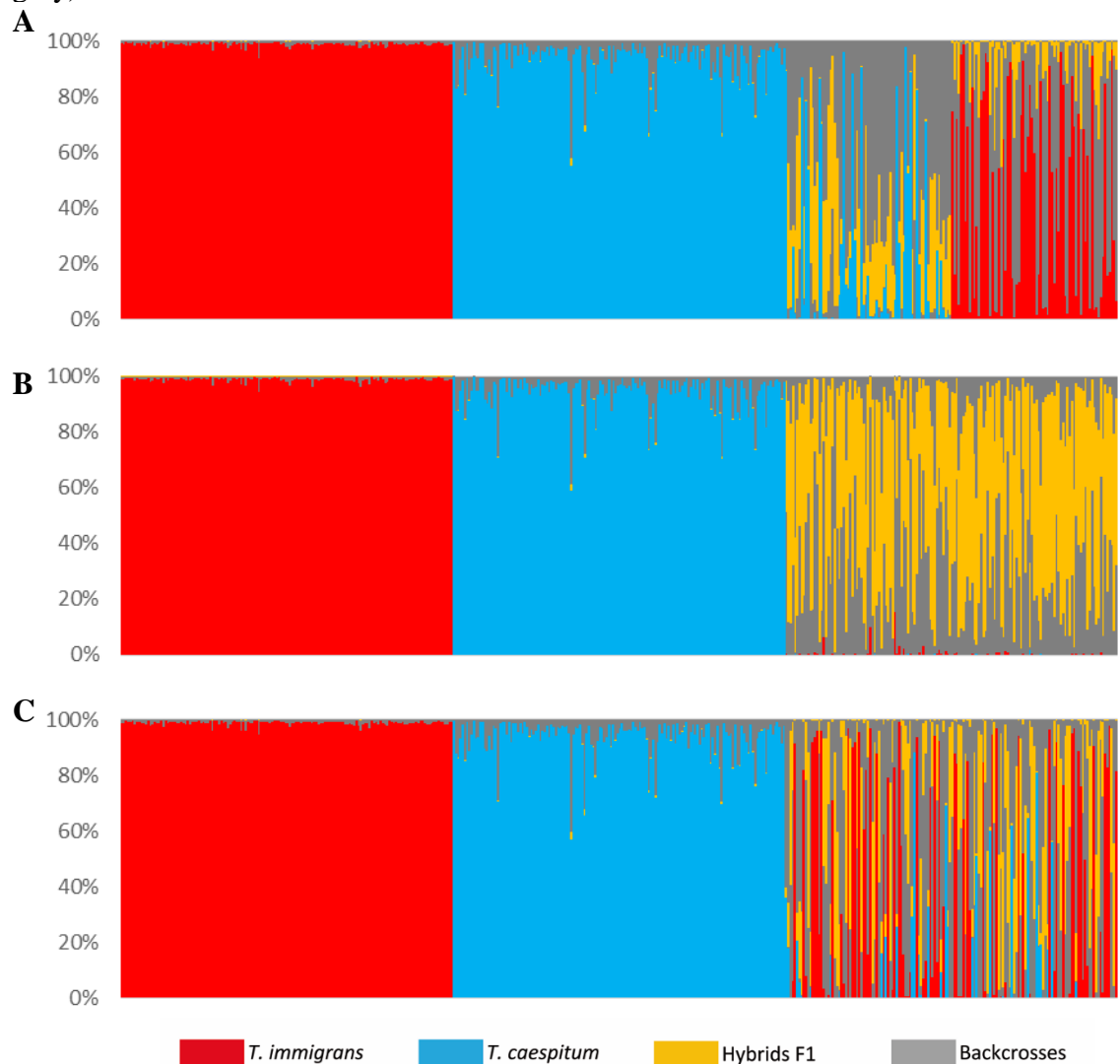


Figure S3. Global relationships of haplotypes based on COI sequences generated in this study and compared to reference sequences obtained from GenBank for *Tetramorium immigrans* (in red) and *T. caespitum* (in blue) (sequence names include species names and GenBank accession number). “T.*immigrans*” indicates a genotype from *Tetramorium immigrans*, “T.*caespitum*” indicates a genotype from *T. caespitum*, “BC” indicates a backcross and “hybrid-F1” indicates a genotype of first-generation hybrid. All sequences were aligned using the default options in MUSCLE v3.8.31 as implemented in SeaView v4.2.9. Based on these aligned sequences, the tree has been calculated using the PhyML algorithm with the GTR distance without invariable sites, optimized nucleotide equilibrium frequencies, and tree-searching operations involving best of NNI & SPR. The branch lengths are proportional to estimated divergence along each branch.

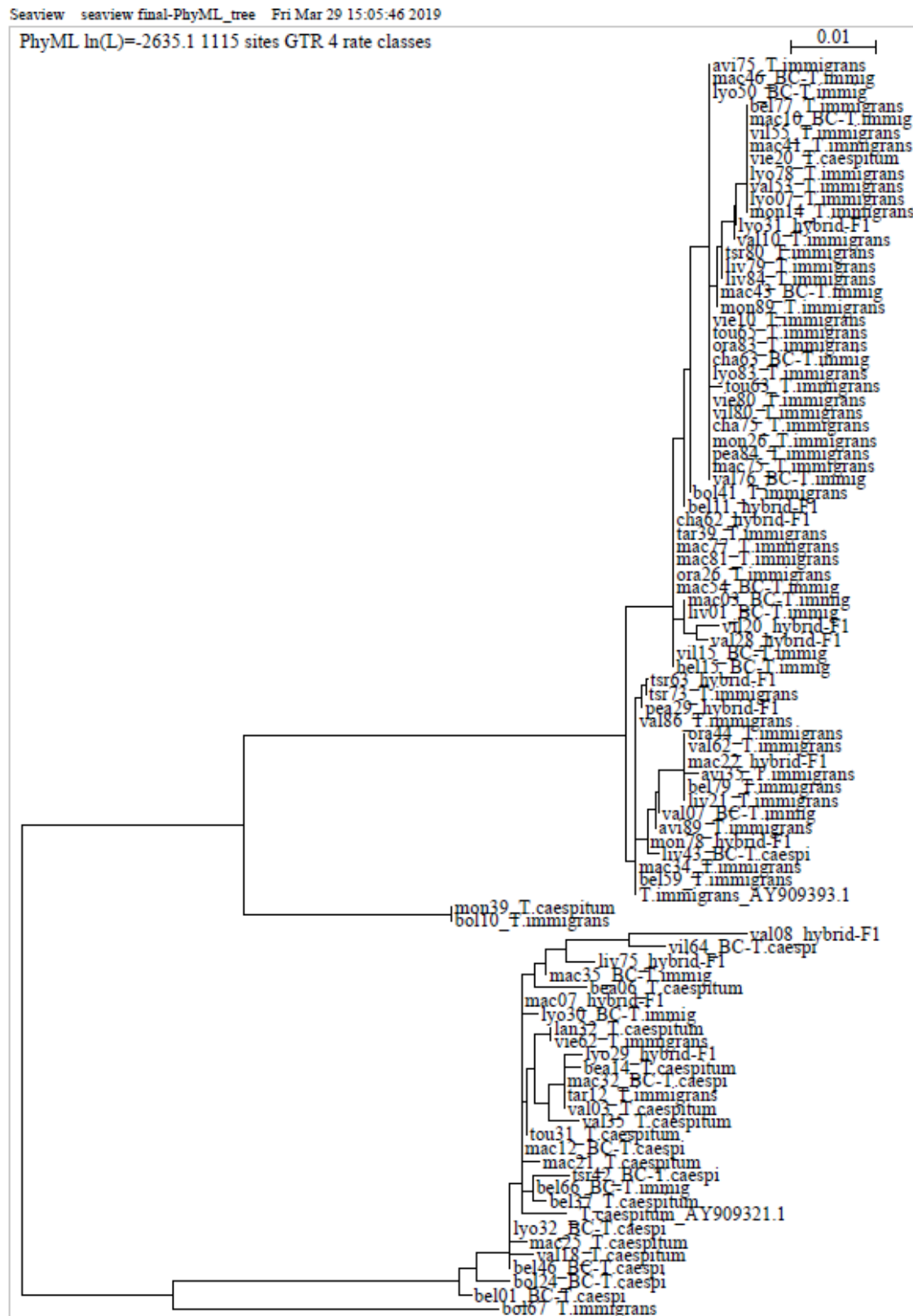


Table S1. GenBank accessions of each sequence used in the study and precise spatial location of associated nests. Accession numbers in italic correspond to sequences used from Cordonnier et al. (2019).

ID	species	Genbank accession	ID	species	Genbank accession	ID	species	Genbank accession
avi_35	<i>T. immigrans</i>	MH398247	lyo_31	hybrid-F1	MK776689	pea_84	<i>T. immigrans</i>	MK776709
avi_75	<i>T. immigrans</i>	MK776668	lyo_32	BC- <i>T. caespi</i>	MK776690	tar_12	<i>T. immigrans</i>	MK776710
avi_89	<i>T. immigrans</i>	MH398250	lyo_50	BC- <i>T. immigrans</i>	MK776691	tar_39	<i>T. immigrans</i>	MH398294
bea_06	<i>T. caespitum</i>	MK776669	lyo_78	<i>T. immigrans</i>	MH398263	tou_31	<i>T. caespitum</i>	MH398295
bea_14	<i>T. caespitum</i>	MH398252	lyo_83	<i>T. immigrans</i>	MH398264	tou_63	<i>T. immigrans</i>	MH398296
bel_01	BC- <i>T. caespi</i>	MK776670	mac_03	BC- <i>T. immigrans</i>	MK776692	tou_65	<i>T. immigrans</i>	MK776711
bel_11	hybrid-F1	MK776671	mac_07	hybrid-F1	MK776693	tsr_42	BC- <i>T. caespi</i>	MK776712
bel_15	BC- <i>T. immigrans</i>	MK776672	mac_10	BC- <i>T. immigrans</i>	MK776694	tsr_63	hybrid-F1	MK776713
bel_37	<i>T. caespitum</i>	MK776673	mac_12	BC- <i>T. caespi</i>	MK776695	tsr_73	<i>T. immigrans</i>	MK776714
bel_46	BC- <i>T. caespi</i>	MK776674	mac_21	<i>T. caespitum</i>	MH398265	tsr_80	<i>T. immigrans</i>	MK776715
bel_59	<i>T. immigrans</i>	MH398253	mac_22	hybrid-F1	MK776696	val_03	<i>T. caespitum</i>	MH398297
bel_66	BC- <i>T. immigrans</i>	MK776675	mac_25	<i>T. caespitum</i>	MH398266	val_07	BC- <i>T. immigrans</i>	MK776716
bel_77	<i>T. immigrans</i>	MK776676	mac_32	BC- <i>T. caespi</i>	MK776697	val_08	hybrid-F1	MK776717
bel_79	<i>T. immigrans</i>	MH398254	mac_34	<i>T. immigrans</i>	MH398267	val_10	<i>T. immigrans</i>	MH398298
bol_10	<i>T. immigrans</i>	MK776677	mac_35	BC- <i>T. immigrans</i>	MK776698	val_18	<i>T. caespitum</i>	MH398299
bol_24	BC- <i>T. caespi</i>	MK776678	mac_41	<i>T. immigrans</i>	MK776699	val_28	hybrid-F1	MK776718
bol_41	<i>T. immigrans</i>	MH398257	mac_43	BC- <i>T. immigrans</i>	MK776700	val_35	<i>T. caespitum</i>	MH398300
bol_67	<i>T. immigrans</i>	MK776679	mac_46	BC- <i>T. immigrans</i>	MK776701	val_53	<i>T. immigrans</i>	MK776719
cha_62	hybrid-F1	MK776680	mac_54	BC- <i>T. immigrans</i>	MK776702	val_62	<i>T. immigrans</i>	MK776720
cha_63	BC- <i>T. immigrans</i>	MK776681	mac_75	<i>T. immigrans</i>	MH398268	val_76	BC- <i>T. immigrans</i>	MK776721
cha_75	<i>T. immigrans</i>	MK776682	mac_77	<i>T. immigrans</i>	MK776703	val_86	<i>T. immigrans</i>	MK776722
lan_32	<i>T. caespitum</i>	MH398259	mac_81	<i>T. immigrans</i>	MH398269	vie_10	<i>T. immigrans</i>	MK776723
liv_01	BC- <i>T. immigrans</i>	MK776683	mon_14	<i>T. immigrans</i>	MH398271	vie_20	<i>T. caespitum</i>	MH398301
liv_21	<i>T. immigrans</i>	MH398260	mon_26	<i>T. immigrans</i>	MK776704	vie_62	<i>T. immigrans</i>	MK776724
liv_43	BC- <i>T. caespi</i>	MK776684	mon_39	<i>T. caespitum</i>	MH398274	vie_80	<i>T. immigrans</i>	MK776725
liv_75	hybrid-F1	MK776685	mon_78	hybrid-F1	MK776705	vil_15	BC- <i>T. immigrans</i>	MK776726
liv_79	<i>T. immigrans</i>	MH398261	mon_89	<i>T. immigrans</i>	MK776706	vil_20	hybrid-F1	MK776727
liv_84	<i>T. immigrans</i>	MK776686	ora_26	<i>T. immigrans</i>	MH398282	vil_55	<i>T. immigrans</i>	MH398302
lyo_07	<i>T. immigrans</i>	MH398262	ora_44	<i>T. immigrans</i>	MH398284	vil_64	BC- <i>T. caespi</i>	MK776728
lyo_29	hybrid-F1	MK776687	ora_83	<i>T. immigrans</i>	MK776707	vil_80	<i>T. immigrans</i>	MK776729
lyo_30	BC- <i>T. immigrans</i>	MK776688	pea_29	hybrid-F1	MK776708			

Cordonnier, M., Bellec, A., Dumet, A., Escarguel, G., & Kaufmann, B. (2018) Range limits in sympatric cryptic species: a case study in *Tetramorium* pavement ants (Hymenoptera: Formicidae) across a biogeographical boundary. *Insect Conservation and Diversity*, 12(2), 109-120.

Table S2. Results of STRUCTURE analyses. Each run consisted in 500.000 replicates of the MCMC after a burn-in of 500.000 replicates. For each K-value, clustering results of 10 independent runs were analyzed using CLUMPAK (Kopelman et al., 2015) based on a Markov clustering algorithm which identifies sets of highly similar runs grouped together in modes and separating these distinct groups of runs to generate a consensus solution for each distinct mode. For any given K, the different runs were either consensual with a single mode or resulting in both a majority mode consisting of most of the iterations and one or more minority modes consisting of the remaining iterations. Structure Harvester (Earl & vonHoldt, 2012) was finally used to identify an optimal ordering of inferred clusters across different values of K, and then to define the optimal K-value using the method of Evanno et al. (2005).

	K=1	K=2	K=3	K=4
Delta K (Structure Harvester)	-	2481.9731	0.3678	-
Division of runs by mode (Clumpak)	-	10/10	8/10, 2/10	9/10, 1/10

- Earl, D.A. (2012) STRUCTURE HARVESTER: a website and program for visualizing STRUCTURE output and implementing the Evanno method. *Conservation genetics resources*, 4, 359-361.
- Kopelman, N.M., Mayzel, J., Jakobsson, M., Rosenberg, N.A., & Mayrose, I. (2015) Clumpak: a program for identifying clustering modes and packaging population structure inferences across K. *Molecular ecology resources*, 15, 1179-1191.
- Evanno, G., Regnaut, S., & Goudet, J. (2005) Detecting the number of clusters of individuals using the software STRUCTURE: a simulation study. *Molecular ecology*, 14, 2611-2620.

Table S3. Results of assignments obtained based on the real data from STRUCTURE, *Snapclust* and NEWHYBRIDS. Each line corresponds to an individual. ID: Sample identity; TI: *Tetramorium immigrans*; TC: *Tetramorium caespitum*; H: Hybrids; HF1: Hybrids F1; HBCI: Hybrids backcrossed with *T. immigrans*; HBCC: Hybrids backcrossed with *T.caespitum*

ID	STRUCTURE		<i>Snapclust</i>			NEWHYBRIDS				
	TI	TC	TI	TC	H	TI	TC	HF1	HBCI	HBCC
avi_01	0.9900	0.0100	1.0000	0.0000	0.0000	0.9978	0.0000	0.0000	0.0022	0.0000
avi_03	0.9910	0.0090	1.0000	0.0000	0.0000	0.9979	0.0000	0.0000	0.0021	0.0000
avi_05	0.9890	0.0110	0.9999	0.0000	0.0001	0.9944	0.0000	0.0000	0.0056	0.0000
avi_08	0.9890	0.0110	0.9999	0.0000	0.0001	0.9945	0.0000	0.0000	0.0055	0.0000
avi_14	0.9908	0.0092	1.0000	0.0000	0.0000	0.9995	0.0000	0.0000	0.0006	0.0000
avi_18	0.9910	0.0090	1.0000	0.0000	0.0000	0.9977	0.0000	0.0000	0.0023	0.0000
avi_20	0.9930	0.0070	1.0000	0.0000	0.0000	0.9996	0.0000	0.0000	0.0004	0.0000
avi_22	0.9922	0.0078	1.0000	0.0000	0.0000	0.9993	0.0000	0.0000	0.0007	0.0000
avi_27	0.9920	0.0080	1.0000	0.0000	0.0000	0.9992	0.0000	0.0000	0.0008	0.0000
avi_33	0.9815	0.0185	1.0000	0.0000	0.0000	0.9791	0.0000	0.0000	0.0209	0.0000
avi_35	0.9891	0.0109	0.9999	0.0000	0.0001	0.9956	0.0000	0.0000	0.0044	0.0000
avi_41	0.9865	0.0135	0.9999	0.0000	0.0001	0.9963	0.0000	0.0000	0.0037	0.0000
avi_45	0.9910	0.0090	1.0000	0.0000	0.0000	0.9988	0.0000	0.0000	0.0013	0.0000
avi_51	0.9930	0.0070	1.0000	0.0000	0.0000	0.9996	0.0000	0.0000	0.0004	0.0000
avi_56	0.9930	0.0070	1.0000	0.0000	0.0000	0.9995	0.0000	0.0000	0.0006	0.0000
avi_61	0.9910	0.0090	0.9999	0.0000	0.0001	0.9982	0.0000	0.0000	0.0018	0.0000
avi_68	0.9920	0.0080	1.0000	0.0000	0.0000	0.9990	0.0000	0.0000	0.0010	0.0000
avi_70	0.9900	0.0100	1.0000	0.0000	0.0000	0.9959	0.0000	0.0000	0.0041	0.0000
avi_73	0.9890	0.0110	1.0000	0.0000	0.0000	0.9985	0.0000	0.0000	0.0015	0.0000
avi_75	0.9920	0.0080	1.0000	0.0000	0.0000	0.9987	0.0000	0.0000	0.0014	0.0000
avi_78	0.9900	0.0100	0.9999	0.0000	0.0001	0.9971	0.0000	0.0000	0.0029	0.0000
avi_83	0.9900	0.0100	1.0000	0.0000	0.0000	0.9964	0.0000	0.0000	0.0036	0.0000
avi_85	0.9790	0.0210	1.0000	0.0000	0.0000	0.9911	0.0000	0.0000	0.0089	0.0000
avi_87	0.9916	0.0084	1.0000	0.0000	0.0000	0.9984	0.0000	0.0000	0.0016	0.0000
avi_90	0.9910	0.0090	1.0000	0.0000	0.0000	0.9972	0.0000	0.0000	0.0028	0.0000
bea_04	0.0060	0.9940	0.0000	1.0000	0.0000	0.0000	0.9999	0.0000	0.0000	0.0001
bea_08	0.0250	0.9750	0.0000	0.9981	0.0019	0.0000	0.9539	0.0000	0.0000	0.0461
bea_17	0.0234	0.9766	0.0000	0.9940	0.0060	0.0000	0.9378	0.0000	0.0000	0.0622
bea_19	0.0180	0.9820	0.0000	0.9996	0.0004	0.0000	0.9930	0.0000	0.0000	0.0070
bea_22	0.0080	0.9920	0.0000	0.9999	0.0001	0.0000	0.9993	0.0000	0.0000	0.0007
bea_34	0.0220	0.9780	0.0000	0.9954	0.0046	0.0000	0.9612	0.0000	0.0000	0.0388
bea_37	0.0070	0.9930	0.0000	1.0000	0.0000	0.0000	0.9998	0.0000	0.0000	0.0002
bea_40	0.0165	0.9835	0.0000	0.9969	0.0031	0.0000	0.9860	0.0000	0.0000	0.0140
bea_43	0.0129	0.9871	0.0000	0.9986	0.0014	0.0000	0.9939	0.0000	0.0000	0.0061
bea_46	0.0060	0.9940	0.0000	1.0000	0.0000	0.0000	0.9999	0.0000	0.0000	0.0001
bea_52	0.0160	0.9840	0.0000	0.9989	0.0011	0.0000	0.9891	0.0000	0.0000	0.0109
bea_55	0.0125	0.9875	0.0000	0.9989	0.0011	0.0000	0.9948	0.0000	0.0000	0.0052
bea_57	0.0070	0.9930	0.0000	1.0000	0.0000	0.0000	0.9997	0.0000	0.0000	0.0003
bea_60	0.0060	0.9940	0.0000	1.0000	0.0000	0.0000	0.9999	0.0000	0.0000	0.0001
bea_64	0.0192	0.9808	0.0000	0.9983	0.0017	0.0000	0.9878	0.0000	0.0000	0.0122
bea_68	0.0151	0.9849	0.0000	0.9962	0.0038	0.0000	0.9949	0.0000	0.0000	0.0051
bea_74	0.0150	0.9850	0.0000	0.9996	0.0004	0.0000	0.9919	0.0000	0.0000	0.0081
bea_76	0.0161	0.9839	0.0000	0.9983	0.0017	0.0000	0.9898	0.0000	0.0000	0.0102
bea_81	0.0090	0.9910	0.0000	0.9999	0.0001	0.0000	0.9992	0.0000	0.0000	0.0008
bea_84	0.0090	0.9910	0.0000	0.9997	0.0003	0.0000	0.9987	0.0000	0.0000	0.0013
bea_86	0.0421	0.9579	0.0000	0.9945	0.0055	0.0000	0.9228	0.0000	0.0000	0.0772
bel_10	0.0070	0.9930	0.0000	1.0000	0.0000	0.0000	0.9997	0.0000	0.0000	0.0003
bel_21	0.0070	0.9930	0.0000	1.0000	0.0000	0.0000	0.9998	0.0000	0.0000	0.0002
bel_24	0.0070	0.9930	0.0000	1.0000	0.0000	0.0000	0.9997	0.0000	0.0000	0.0003
bel_33	0.0140	0.9860	0.0000	0.9995	0.0005	0.0000	0.9940	0.0000	0.0000	0.0060
bel_37	0.0060	0.9940	0.0000	1.0000	0.0000	0.0000	0.9999	0.0000	0.0000	0.0001

bel_40	0.0247	0.9753	0.0000	0.9998	0.0002	0.0000	0.9820	0.0000	0.0000	0.0180
bel_72	0.0073	0.9927	0.0000	1.0000	0.0000	0.0000	0.9996	0.0000	0.0000	0.0004
bel_76	0.0080	0.9920	0.0000	0.9999	0.0001	0.0000	0.9994	0.0000	0.0000	0.0006
bel_82	0.0100	0.9900	0.0000	0.9993	0.0007	0.0000	0.9982	0.0000	0.0000	0.0018
bel_84	0.0074	0.9926	0.0000	1.0000	0.0000	0.0000	0.9996	0.0000	0.0000	0.0004
bel_86	0.0130	0.9870	0.0000	0.9997	0.0003	0.0000	0.9975	0.0000	0.0000	0.0025
bol_02	0.9879	0.0121	1.0000	0.0000	0.0000	0.9961	0.0000	0.0000	0.0040	0.0000
bol_10	0.9760	0.0240	1.0000	0.0000	0.0000	0.9861	0.0000	0.0000	0.0139	0.0000
bol_13	0.9930	0.0070	1.0000	0.0000	0.0000	0.9994	0.0000	0.0000	0.0006	0.0000
bol_16	0.9921	0.0079	1.0000	0.0000	0.0000	0.9991	0.0000	0.0000	0.0009	0.0000
bol_20	0.9790	0.0210	0.9999	0.0000	0.0001	0.9792	0.0000	0.0000	0.0208	0.0000
bol_30	0.9800	0.0200	1.0000	0.0000	0.0000	0.9796	0.0000	0.0000	0.0204	0.0000
bol_32	0.9910	0.0090	0.9999	0.0000	0.0001	0.9976	0.0000	0.0000	0.0024	0.0000
bol_33	0.9930	0.0070	1.0000	0.0000	0.0000	0.9997	0.0000	0.0000	0.0003	0.0000
bol_35	0.9890	0.0110	0.9999	0.0000	0.0001	0.9946	0.0000	0.0000	0.0054	0.0000
bol_36	0.9930	0.0070	1.0000	0.0000	0.0000	0.9993	0.0000	0.0000	0.0007	0.0000
bol_39	0.9801	0.0199	1.0000	0.0000	0.0000	0.9940	0.0000	0.0000	0.0060	0.0000
bol_41	0.9931	0.0069	1.0000	0.0000	0.0000	0.9997	0.0000	0.0000	0.0003	0.0000
bol_52	0.9694	0.0306	0.9999	0.0000	0.0001	0.9581	0.0000	0.0000	0.0419	0.0000
bol_55	0.9900	0.0100	1.0000	0.0000	0.0000	0.9978	0.0000	0.0000	0.0022	0.0000
bol_59	0.9900	0.0100	1.0000	0.0000	0.0000	0.9966	0.0000	0.0000	0.0034	0.0000
bol_63	0.9691	0.0309	0.9999	0.0000	0.0001	0.9713	0.0000	0.0000	0.0288	0.0000
bol_66	0.9691	0.0309	0.9998	0.0000	0.0002	0.9040	0.0000	0.0000	0.0960	0.0000
bol_68	0.9840	0.0160	0.9999	0.0000	0.0001	0.9897	0.0000	0.0000	0.0103	0.0000
bol_70	0.9940	0.0060	1.0000	0.0000	0.0000	0.9998	0.0000	0.0000	0.0003	0.0000
bol_74	0.9850	0.0150	0.9999	0.0000	0.0001	0.9930	0.0000	0.0000	0.0070	0.0000
bol_76	0.9727	0.0273	1.0000	0.0000	0.0000	0.9794	0.0000	0.0000	0.0206	0.0000
bol_85	0.9900	0.0100	1.0000	0.0000	0.0000	0.9965	0.0000	0.0000	0.0035	0.0000
bol_87	0.9895	0.0105	0.9999	0.0000	0.0001	0.9966	0.0000	0.0000	0.0034	0.0000
bol_89	0.9897	0.0103	0.9999	0.0000	0.0001	0.9960	0.0000	0.0000	0.0040	0.0000
cha_04	0.0060	0.9940	0.0000	1.0000	0.0000	0.0000	0.9999	0.0000	0.0000	0.0001
cha_08	0.0121	0.9879	0.0000	0.9998	0.0002	0.0000	0.9919	0.0000	0.0000	0.0081
cha_11	0.0119	0.9881	0.0000	0.9979	0.0021	0.0000	0.9951	0.0000	0.0000	0.0049
cha_16	0.0110	0.9890	0.0000	0.9994	0.0006	0.0000	0.9952	0.0000	0.0000	0.0048
cha_19	0.0140	0.9860	0.0000	0.9995	0.0005	0.0000	0.9930	0.0000	0.0000	0.0071
cha_20	0.0117	0.9883	0.0000	0.9995	0.0005	0.0000	0.9974	0.0000	0.0000	0.0026
cha_25	0.0080	0.9920	0.0000	0.9999	0.0001	0.0000	0.9995	0.0000	0.0000	0.0005
cha_28	0.0338	0.9662	0.0000	0.9988	0.0012	0.0000	0.9179	0.0000	0.0000	0.0821
cha_33	0.0120	0.9880	0.0000	0.9995	0.0005	0.0000	0.9955	0.0000	0.0000	0.0045
cha_37	0.0100	0.9900	0.0000	0.9994	0.0006	0.0000	0.9985	0.0000	0.0000	0.0015
cha_43	0.0090	0.9910	0.0000	0.9999	0.0001	0.0000	0.9986	0.0000	0.0000	0.0014
cha_51	0.0135	0.9865	0.0000	0.9989	0.0011	0.0000	0.9920	0.0000	0.0000	0.0080
cha_55	0.0080	0.9920	0.0000	0.9999	0.0001	0.0000	0.9994	0.0000	0.0000	0.0006
cha_60	0.0179	0.9821	0.0000	0.9998	0.0002	0.0000	0.9847	0.0000	0.0000	0.0153
cha_65	0.0130	0.9870	0.0000	0.9993	0.0007	0.0000	0.9963	0.0000	0.0000	0.0037
cha_70	0.0090	0.9910	0.0000	0.9998	0.0002	0.0000	0.9988	0.0000	0.0000	0.0012
cha_73	0.0110	0.9890	0.0000	0.9999	0.0001	0.0000	0.9984	0.0000	0.0000	0.0016
cha_77	0.0100	0.9900	0.0000	0.9999	0.0001	0.0000	0.9977	0.0000	0.0000	0.0023
cha_79	0.0099	0.9901	0.0000	0.9999	0.0001	0.0000	0.9991	0.0000	0.0000	0.0009
cha_85	0.0089	0.9911	0.0000	0.9998	0.0002	0.0000	0.9992	0.0000	0.0000	0.0008
cha_88	0.0130	0.9870	0.0000	0.9990	0.0010	0.0000	0.9928	0.0000	0.0000	0.0072
dij_03	0.0616	0.9384	0.0000	0.9658	0.0342	0.0000	0.6634	0.0000	0.0000	0.3366
dij_06	0.0120	0.9880	0.0000	0.9995	0.0005	0.0000	0.9961	0.0000	0.0000	0.0040
dij_09	0.0100	0.9900	0.0000	0.9998	0.0002	0.0000	0.9984	0.0000	0.0000	0.0016
dij_12	0.0110	0.9890	0.0000	0.9997	0.0003	0.0000	0.9984	0.0000	0.0000	0.0016
dij_16	0.0080	0.9920	0.0000	0.9999	0.0001	0.0000	0.9990	0.0000	0.0000	0.0010
dij_23	0.0150	0.9850	0.0000	0.9981	0.0019	0.0000	0.9900	0.0000	0.0000	0.0100
dij_30	0.0358	0.9642	0.0000	0.9690	0.0310	0.0000	0.9359	0.0000	0.0000	0.0641
dij_34	0.0120	0.9880	0.0000	0.9997	0.0003	0.0000	0.9947	0.0000	0.0000	0.0053

dij_42	0.0080	0.9920	0.0000	0.9999	0.0001	0.0000	0.9994	0.0000	0.0000	0.0000	0.0006
dij_46	0.0207	0.9793	0.0000	0.9993	0.0007	0.0000	0.9914	0.0000	0.0000	0.0000	0.0087
dij_49	0.0144	0.9856	0.0000	0.9949	0.0051	0.0000	0.9898	0.0000	0.0000	0.0000	0.0102
dij_53	0.0310	0.9690	0.0000	0.9903	0.0097	0.0000	0.9338	0.0000	0.0000	0.0000	0.0662
dij_57	0.0131	0.9869	0.0000	0.9982	0.0018	0.0000	0.9921	0.0000	0.0000	0.0000	0.0079
dij_60	0.0090	0.9910	0.0000	0.9998	0.0002	0.0000	0.9990	0.0000	0.0000	0.0000	0.0010
dij_63	0.0100	0.9900	0.0000	0.9996	0.0004	0.0000	0.9980	0.0000	0.0000	0.0000	0.0020
dij_67	0.0171	0.9829	0.0000	0.9992	0.0008	0.0000	0.9941	0.0000	0.0000	0.0000	0.0059
dij_70	0.0120	0.9880	0.0000	0.9987	0.0013	0.0000	0.9970	0.0000	0.0000	0.0000	0.0030
dij_77	0.0080	0.9920	0.0000	0.9999	0.0001	0.0000	0.9993	0.0000	0.0000	0.0000	0.0007
dij_83	0.0230	0.9770	0.0000	0.9978	0.0022	0.0000	0.9732	0.0000	0.0000	0.0000	0.0268
dij_86	0.0090	0.9910	0.0000	0.9999	0.0001	0.0000	0.9990	0.0000	0.0000	0.0000	0.0011
dij_90	0.0136	0.9864	0.0000	0.9982	0.0018	0.0000	0.9958	0.0000	0.0000	0.0000	0.0042
bel_01	0.0793	0.9207	0.0000	0.9620	0.0380	0.0000	0.4797	0.0000	0.0000	0.0000	0.5203
bel_06	0.1733	0.8267	0.0000	0.8465	0.1535	0.0000	0.0029	0.0003	0.0000	0.0000	0.9969
bel_11	0.5027	0.4973	0.0099	0.0000	0.9901	0.0000	0.0000	0.9562	0.0325	0.0112	
bel_12	0.6049	0.3951	0.5852	0.0000	0.4148	0.0000	0.0000	0.0662	0.9331	0.0007	
bel_15	0.9282	0.0718	0.9992	0.0000	0.0008	0.2183	0.0000	0.0000	0.7817	0.0000	
bel_20	0.1489	0.8511	0.0000	0.8624	0.1376	0.0000	0.0060	0.0000	0.0000	0.0000	0.9940
bel_26	0.2571	0.7429	0.0000	0.2235	0.7765	0.0000	0.0000	0.4570	0.0032	0.5397	
bel_29	0.2868	0.7132	0.0000	0.0325	0.9675	0.0000	0.0000	0.0000	0.0000	0.0000	1.0000
bel_30	0.8337	0.1663	0.9919	0.0000	0.0081	0.0100	0.0000	0.0000	0.9900	0.0000	
bel_34	0.6762	0.3238	0.6477	0.0000	0.3523	0.0000	0.0000	0.2022	0.7972	0.0006	
bel_43	0.4757	0.5243	0.0041	0.0014	0.9946	0.0000	0.0000	0.3429	0.0208	0.6364	
bel_46	0.1987	0.8013	0.0000	0.2225	0.7775	0.0000	0.0055	0.0001	0.0000	0.0000	0.9944
bel_48	0.9552	0.0448	0.9997	0.0000	0.0003	0.6049	0.0000	0.0000	0.3952	0.0000	
bel_51	0.9255	0.0745	0.9989	0.0000	0.0011	0.2967	0.0000	0.0000	0.7033	0.0000	
bel_53	0.9741	0.0259	0.9997	0.0000	0.0003	0.7721	0.0000	0.0000	0.2279	0.0000	
bel_55	0.5959	0.4041	0.9409	0.0000	0.0591	0.0000	0.0000	0.2456	0.7537	0.0007	
bel_57	0.9457	0.0543	0.9997	0.0000	0.0003	0.9424	0.0000	0.0000	0.0576	0.0000	
bel_61	0.4816	0.5184	0.0766	0.0024	0.9211	0.0000	0.0000	0.7442	0.1096	0.1462	
bel_63	0.4379	0.5621	0.0271	0.0004	0.9725	0.0000	0.0000	0.0726	0.0109	0.9166	
bel_66	0.6329	0.3671	0.0626	0.0000	0.9373	0.0000	0.0000	0.1971	0.8027	0.0002	
bel_67	0.1235	0.8765	0.0000	0.6586	0.3414	0.0000	0.3154	0.0051	0.0000	0.6795	
bel_68	0.7723	0.2277	0.9892	0.0000	0.0108	0.0001	0.0000	0.0000	0.9999	0.0000	
bel_80	0.4427	0.5573	0.0001	0.0001	0.9997	0.0000	0.0000	0.5345	0.0542	0.4114	
bol_24	0.3634	0.6366	0.0000	0.0076	0.9924	0.0000	0.0000	0.0359	0.0002	0.9639	
cha_30	0.2677	0.7323	0.0000	0.0831	0.9169	0.0000	0.0000	0.0000	0.0000	0.0000	1.0000
cha_58	0.7151	0.2849	0.9545	0.0000	0.0455	0.0000	0.0000	0.0000	1.0000	0.0000	
cha_61	0.5938	0.4062	0.2337	0.0000	0.7663	0.0000	0.0000	0.0001	0.9999	0.0000	
cha_62	0.4773	0.5227	0.0003	0.0000	0.9997	0.0000	0.0000	0.8166	0.0359	0.1474	
cha_63	0.9729	0.0271	0.9996	0.0000	0.0004	0.8992	0.0000	0.0000	0.1008	0.0000	
cha_69	0.5079	0.4921	0.0006	0.0000	0.9994	0.0000	0.0000	0.9566	0.0343	0.0091	
cha_78	0.8242	0.1758	0.9992	0.0000	0.0008	0.0001	0.0000	0.0000	0.9999	0.0000	
cha_82	0.9289	0.0711	0.9984	0.0000	0.0016	0.0707	0.0000	0.0000	0.9293	0.0000	
liv_06	0.5560	0.4440	0.0151	0.0000	0.9849	0.0000	0.0000	0.8798	0.1195	0.0008	
liv_07	0.9535	0.0465	0.9995	0.0000	0.0005	0.8460	0.0000	0.0000	0.1540	0.0000	
liv_43	0.4475	0.5525	0.0009	0.0017	0.9974	0.0000	0.0000	0.0150	0.0151	0.9699	
liv_46	0.7884	0.2116	0.9831	0.0000	0.0169	0.0001	0.0000	0.0000	0.9999	0.0000	
liv_62	0.7600	0.2400	0.9961	0.0000	0.0039	0.0001	0.0000	0.0000	0.9999	0.0000	
liv_75	0.6011	0.3989	0.8587	0.0000	0.1413	0.0000	0.0000	0.5240	0.4754	0.0006	
lyo_02	0.9211	0.0789	0.9998	0.0000	0.0002	0.1561	0.0000	0.0000	0.8439	0.0000	
lyo_14	0.3547	0.6453	0.0002	0.0032	0.9965	0.0000	0.0000	0.0031	0.0000	0.9968	
lyo_26	0.4661	0.5339	0.0004	0.0000	0.9996	0.0000	0.0000	0.8077	0.0983	0.0940	
lyo_30	0.8021	0.1979	0.9982	0.0000	0.0018	0.0001	0.0000	0.0001	0.9998	0.0000	
lyo_31	0.5405	0.4595	0.0067	0.0000	0.9933	0.0000	0.0000	0.6599	0.1021	0.2380	
lyo_32	0.1772	0.8228	0.0000	0.9061	0.0939	0.0000	0.0473	0.0000	0.0000	0.9527	
lyo_33	0.7448	0.2552	0.9671	0.0000	0.0329	0.0000	0.0000	0.0000	1.0000	0.0000	
lyo_39	0.1663	0.8337	0.0000	0.8869	0.1131	0.0000	0.0000	0.0000	0.0000	1.0000	

lyo_42	0.7319	0.2681	0.9959	0.0000	0.0041	0.0000	0.0000	0.0001	0.9999	0.0000
lyo_46	0.3969	0.6031	0.0035	0.0006	0.9959	0.0000	0.0000	0.7789	0.0078	0.2133
lyo_49	0.7046	0.2954	0.5380	0.0000	0.4620	0.0000	0.0000	0.0000	1.0000	0.0000
lyo_50	0.8765	0.1235	0.9981	0.0000	0.0019	0.0009	0.0000	0.0000	0.9991	0.0000
lyo_53	0.1066	0.8934	0.0000	0.9334	0.0666	0.0000	0.0367	0.0000	0.0000	0.9633
lyo_87	0.9770	0.0230	1.0000	0.0000	0.0000	0.9216	0.0000	0.0000	0.0784	0.0000
mac_03	0.7702	0.2298	0.9830	0.0000	0.0170	0.0000	0.0000	0.0013	0.9987	0.0000
mac_04	0.6337	0.3663	0.8519	0.0000	0.1481	0.0000	0.0000	0.8117	0.1869	0.0014
mac_07	0.6050	0.3950	0.0431	0.0001	0.9568	0.0000	0.0000	0.5838	0.4054	0.0108
mac_08	0.5030	0.4970	0.0147	0.0037	0.9816	0.0000	0.0000	0.7955	0.1700	0.0346
mac_10	0.6897	0.3103	0.7942	0.0000	0.2058	0.0000	0.0000	0.0462	0.9535	0.0003
mac_12	0.0814	0.9186	0.0000	0.8774	0.1226	0.0000	0.1023	0.0000	0.0000	0.8977
mac_14	0.0270	0.9730	0.0000	0.9943	0.0057	0.0000	0.3893	0.0000	0.0000	0.6107
mac_16	0.9137	0.0863	0.9996	0.0000	0.0004	0.0105	0.0000	0.0000	0.9895	0.0000
mac_17	0.1675	0.8325	0.0000	0.8626	0.1374	0.0000	0.0001	0.0000	0.0000	0.9999
mac_22	0.3160	0.6840	0.0001	0.0528	0.9471	0.0000	0.0000	0.6180	0.0090	0.3730
mac_28	0.5464	0.4536	0.6944	0.0000	0.3056	0.0000	0.0000	0.2508	0.6264	0.1228
mac_30	0.6732	0.3268	0.8073	0.0000	0.1927	0.0000	0.0000	0.0183	0.9815	0.0003
mac_32	0.1108	0.8892	0.0000	0.9287	0.0713	0.0000	0.4300	0.0000	0.0000	0.5700
mac_35	0.8124	0.1876	0.9881	0.0000	0.0119	0.0005	0.0000	0.0002	0.9993	0.0000
mac_36	0.6186	0.3814	0.5319	0.0000	0.4681	0.0000	0.0000	0.1182	0.8810	0.0009
mac_40	0.9476	0.0524	0.9994	0.0000	0.0006	0.3952	0.0000	0.0000	0.6048	0.0000
mac_44	0.5587	0.4413	0.6676	0.0000	0.3324	0.0000	0.0000	0.0317	0.9671	0.0012
mac_46	0.8576	0.1424	0.9989	0.0000	0.0011	0.4476	0.0000	0.0000	0.5524	0.0000
mac_52	0.1870	0.8130	0.0000	0.6929	0.3071	0.0000	0.0186	0.0000	0.0000	0.9814
mac_54	0.8377	0.1623	0.9423	0.0000	0.0577	0.0024	0.0000	0.0000	0.9976	0.0000
mac_55	0.0411	0.9589	0.0000	0.9790	0.0210	0.0000	0.6830	0.0000	0.0000	0.3170
mac_59	0.1085	0.8915	0.0000	0.9044	0.0956	0.0000	0.4837	0.0000	0.0000	0.5163
mac_68	0.5582	0.4418	0.0078	0.0000	0.9922	0.0000	0.0000	0.8402	0.1525	0.0073
mac_73	0.5933	0.4067	0.0308	0.0000	0.9692	0.0000	0.0000	0.5315	0.4665	0.0021
mac_83	0.8706	0.1294	0.9978	0.0000	0.0022	0.0019	0.0000	0.0000	0.9981	0.0000
mac_85	0.8082	0.1918	0.9954	0.0000	0.0046	0.0006	0.0000	0.0001	0.9993	0.0000
mon_05	0.5601	0.4399	0.0320	0.0000	0.9680	0.0000	0.0000	0.8019	0.1870	0.0112
mon_57	0.5187	0.4813	0.0848	0.0001	0.9151	0.0000	0.0000	0.7086	0.1637	0.1278
mon_63	0.7369	0.2631	0.9914	0.0000	0.0086	0.0000	0.0000	0.0003	0.9997	0.0000
mon_78	0.4622	0.5378	0.0023	0.0005	0.9972	0.0000	0.0000	0.9427	0.0185	0.0388
mon_86	0.8275	0.1725	0.9982	0.0000	0.0018	0.0002	0.0000	0.0000	0.9998	0.0000
ora_68	0.8199	0.1801	0.9636	0.0000	0.0364	0.0000	0.0000	0.0000	1.0000	0.0000
pea_22	0.0962	0.9038	0.0000	0.8364	0.1636	0.0000	0.3572	0.0000	0.0000	0.6429
pea_29	0.4261	0.5739	0.0091	0.0015	0.9894	0.0000	0.0000	0.9162	0.0174	0.0664
pea_33	0.1159	0.8841	0.0000	0.9847	0.0153	0.0000	0.0009	0.0000	0.0000	0.9991
pea_59	0.4835	0.5165	0.0068	0.0000	0.9932	0.0000	0.0000	0.8948	0.0827	0.0225
pea_61	0.5100	0.4900	0.0156	0.0001	0.9843	0.0000	0.0000	0.9034	0.0856	0.0110
pea_66	0.8812	0.1188	0.9982	0.0000	0.0018	0.0012	0.0000	0.0000	0.9988	0.0000
pea_76	0.6444	0.3556	0.2790	0.0000	0.7210	0.0000	0.0000	0.0205	0.9795	0.0000
pea_77	0.3160	0.6840	0.0000	0.0009	0.9991	0.0000	0.0000	0.0007	0.0000	0.9994
pea_78	0.0583	0.9417	0.0000	0.9761	0.0239	0.0000	0.5986	0.0000	0.0000	0.4014
pea_79	0.8620	0.1380	0.9998	0.0000	0.0002	0.0002	0.0000	0.0000	0.9998	0.0000
tou_62	0.5668	0.4332	0.0266	0.0000	0.9733	0.0000	0.0000	0.2648	0.7322	0.0029
tou_68	0.9579	0.0421	0.9998	0.0000	0.0002	0.5567	0.0000	0.0000	0.4433	0.0000
tou_70	0.2817	0.7183	0.0000	0.0152	0.9847	0.0000	0.0000	0.0000	0.0000	1.0000
tou_71	0.5543	0.4457	0.0265	0.0007	0.9727	0.0000	0.0000	0.6764	0.3081	0.0156
tou_79	0.2940	0.7060	0.0000	0.0411	0.9589	0.0000	0.0002	0.0000	0.0000	0.9998
tou_90	0.5826	0.4174	0.5558	0.0000	0.4442	0.0000	0.0000	0.3336	0.3739	0.2925
tsr_14	0.4602	0.5398	0.0033	0.0008	0.9959	0.0000	0.0000	0.8462	0.0659	0.0879
tsr_33	0.3734	0.6266	0.0000	0.0030	0.9970	0.0000	0.0000	0.2921	0.0078	0.7001
tsr_42	0.0638	0.9362	0.0000	0.9833	0.0167	0.0000	0.3362	0.0000	0.0000	0.6638
tsr_58	0.3018	0.6982	0.0001	0.0146	0.9854	0.0000	0.0000	0.0588	0.0001	0.9411
tsr_63	0.3933	0.6067	0.0009	0.0009	0.9982	0.0000	0.0000	0.9603	0.0094	0.0303

tsr_70	0.9421	0.0579	0.9994	0.0000	0.0006	0.2643	0.0000	0.0000	0.7358	0.0000
tsr_78	0.4533	0.5467	0.0052	0.0000	0.9947	0.0000	0.0000	0.5409	0.0057	0.4534
tsr_85	0.7785	0.2215	0.9819	0.0000	0.0181	0.0000	0.0000	0.0000	1.0000	0.0000
tsr_87	0.3738	0.6262	0.0006	0.0034	0.9960	0.0000	0.0000	0.4639	0.1257	0.4104
val_04	0.0570	0.9430	0.0000	0.9796	0.0204	0.0000	0.0870	0.0000	0.0000	0.9130
val_07	0.6458	0.3542	0.2084	0.0000	0.7916	0.0000	0.0000	0.0095	0.9891	0.0014
val_08	0.5019	0.4981	0.0106	0.0000	0.9893	0.0000	0.0000	0.9826	0.0157	0.0017
val_11	0.4378	0.5622	0.0033	0.0001	0.9965	0.0000	0.0000	0.9170	0.0150	0.0680
val_15	0.0461	0.9539	0.0000	0.9903	0.0097	0.0000	0.3473	0.0000	0.0000	0.6527
val_16	0.1218	0.8782	0.0000	0.7989	0.2011	0.0000	0.7289	0.0000	0.0000	0.2711
val_17	0.1322	0.8678	0.0000	0.9493	0.0507	0.0000	0.0045	0.0000	0.0000	0.9955
val_22	0.3373	0.6627	0.0000	0.0030	0.9970	0.0000	0.0000	0.1785	0.0004	0.8211
val_28	0.4704	0.5296	0.0020	0.0002	0.9978	0.0000	0.0000	0.9698	0.0174	0.0128
val_30	0.1639	0.8361	0.0000	0.8306	0.1694	0.0000	0.1146	0.0000	0.0000	0.8854
val_46	0.9028	0.0972	0.9998	0.0000	0.0002	0.0260	0.0000	0.0000	0.9740	0.0000
val_55	0.0764	0.9236	0.0000	0.9866	0.0134	0.0000	0.0651	0.0000	0.0000	0.9350
val_87	0.6291	0.3709	0.8126	0.0000	0.1874	0.0000	0.0000	0.0088	0.9912	0.0000
vie_08	0.8903	0.1097	0.9995	0.0000	0.0005	0.0028	0.0000	0.0000	0.9972	0.0000
vie_25	0.5588	0.4412	0.0125	0.0000	0.9874	0.0000	0.0000	0.9187	0.0790	0.0024
vie_30	0.4519	0.5481	0.0099	0.0010	0.9892	0.0000	0.0000	0.8060	0.1284	0.0656
vie_31	0.8504	0.1496	0.9967	0.0000	0.0033	0.0004	0.0000	0.0000	0.9996	0.0000
vie_36	0.5017	0.4983	0.0003	0.0000	0.9997	0.0000	0.0000	0.9841	0.0131	0.0029
vie_46	0.5241	0.4759	0.0183	0.0000	0.9817	0.0000	0.0000	0.9715	0.0252	0.0033
vie_47	0.5627	0.4373	0.0481	0.0000	0.9519	0.0000	0.0000	0.5266	0.4696	0.0037
vie_65	0.9520	0.0480	0.9997	0.0000	0.0003	0.2582	0.0000	0.0000	0.7418	0.0000
vie_82	0.9544	0.0456	0.9998	0.0000	0.0002	0.4362	0.0000	0.0000	0.5639	0.0000
vil_07	0.1647	0.8353	0.0000	0.5498	0.4502	0.0000	0.0047	0.0000	0.0000	0.9953
vil_13	0.8707	0.1293	0.9995	0.0000	0.0005	0.0001	0.0000	0.0000	0.9999	0.0000
vil_15	0.7480	0.2520	0.9886	0.0000	0.0114	0.0001	0.0000	0.0000	0.9999	0.0000
vil_20	0.5235	0.4765	0.6043	0.0000	0.3957	0.0000	0.0000	0.7341	0.2414	0.0245
vil_23	0.8420	0.1580	0.9778	0.0000	0.0222	0.0001	0.0000	0.0001	0.9998	0.0000
vil_27	0.6469	0.3531	0.7674	0.0000	0.2326	0.0000	0.0000	0.4027	0.5964	0.0009
vil_39	0.4583	0.5417	0.0005	0.0000	0.9995	0.0000	0.0000	0.9587	0.0067	0.0346
vil_43	0.5547	0.4453	0.0006	0.0000	0.9993	0.0000	0.0000	0.6264	0.3622	0.0114
vil_44	0.9100	0.0900	0.9996	0.0000	0.0004	0.0101	0.0000	0.0000	0.9899	0.0000
vil_46	0.3346	0.6654	0.0000	0.0079	0.9921	0.0000	0.0000	0.0010	0.0000	0.9990
vil_47	0.5187	0.4813	0.0010	0.0000	0.9990	0.0000	0.0000	0.2059	0.5715	0.2226
vil_49	0.7214	0.2786	0.9506	0.0000	0.0494	0.0000	0.0000	0.0001	0.9999	0.0000
vil_51	0.5909	0.4091	0.1641	0.0000	0.8359	0.0000	0.0000	0.7592	0.2353	0.0056
vil_53	0.8957	0.1043	0.9985	0.0000	0.0015	0.0013	0.0000	0.0000	0.9987	0.0000
vil_57	0.8189	0.1811	0.9972	0.0000	0.0028	0.0001	0.0000	0.0000	0.9999	0.0000
vil_69	0.9376	0.0624	0.9999	0.0000	0.0001	0.1271	0.0000	0.0000	0.8729	0.0000
vil_70	0.5278	0.4722	0.0050	0.0000	0.9949	0.0000	0.0000	0.8773	0.1175	0.0052
vil_76	0.2947	0.7053	0.0001	0.0084	0.9914	0.0000	0.0000	0.0000	0.0000	1.0000
vil_78	0.8805	0.1195	0.9981	0.0000	0.0019	0.0894	0.0000	0.0000	0.9106	0.0000
lan_02	0.0160	0.9840	0.0000	0.9991	0.0009	0.0000	0.9940	0.0000	0.0000	0.0060
lan_04	0.0110	0.9890	0.0000	0.9998	0.0002	0.0000	0.9953	0.0000	0.0000	0.0047
lan_08	0.0070	0.9930	0.0000	1.0000	0.0000	0.0000	0.9997	0.0000	0.0000	0.0003
lan_14	0.0159	0.9841	0.0000	0.9999	0.0001	0.0000	0.9978	0.0000	0.0000	0.0022
lan_17	0.0142	0.9858	0.0000	0.9999	0.0001	0.0000	0.9957	0.0000	0.0000	0.0043
lan_22	0.0110	0.9890	0.0000	0.9996	0.0004	0.0000	0.9977	0.0000	0.0000	0.0023
lan_28	0.0169	0.9831	0.0000	0.9996	0.0004	0.0000	0.9846	0.0000	0.0000	0.0154
lan_32	0.0070	0.9930	0.0000	1.0000	0.0000	0.0000	0.9997	0.0000	0.0000	0.0003
lan_38	0.0110	0.9890	0.0000	0.9997	0.0003	0.0000	0.9957	0.0000	0.0000	0.0044
lan_42	0.0114	0.9886	0.0000	0.9993	0.0007	0.0000	0.9932	0.0000	0.0000	0.0068
lan_45	0.0070	0.9930	0.0000	1.0000	0.0000	0.0000	0.9998	0.0000	0.0000	0.0002
lan_50	0.0110	0.9890	0.0000	0.9998	0.0002	0.0000	0.9973	0.0000	0.0000	0.0027
lan_60	0.0090	0.9910	0.0000	0.9998	0.0002	0.0000	0.9987	0.0000	0.0000	0.0013
lan_62	0.0140	0.9860	0.0000	0.9989	0.0011	0.0000	0.9934	0.0000	0.0000	0.0066

lan_67	0.0463	0.9537	0.0000	0.9925	0.0075	0.0000	0.8955	0.0000	0.0000	0.1045
lan_69	0.0180	0.9820	0.0000	0.9926	0.0074	0.0000	0.9893	0.0000	0.0000	0.0107
lan_72	0.0170	0.9830	0.0000	0.9990	0.0010	0.0000	0.9820	0.0000	0.0000	0.0180
lan_77	0.0291	0.9709	0.0000	0.9900	0.0100	0.0000	0.9513	0.0000	0.0000	0.0487
lan_83	0.0140	0.9860	0.0000	0.9967	0.0033	0.0000	0.9927	0.0000	0.0000	0.0074
lan_86	0.0080	0.9920	0.0000	0.9999	0.0001	0.0000	0.9992	0.0000	0.0000	0.0008
lan_89	0.0118	0.9882	0.0000	0.9993	0.0007	0.0000	0.9969	0.0000	0.0000	0.0031
liv_10	0.9920	0.0080	1.0000	0.0000	0.0000	0.9988	0.0000	0.0000	0.0012	0.0000
liv_11	0.0070	0.9930	0.0000	1.0000	0.0000	0.0000	0.9997	0.0000	0.0000	0.0003
liv_13	0.0160	0.9840	0.0000	0.9992	0.0008	0.0000	0.9885	0.0000	0.0000	0.0115
liv_17	0.0090	0.9910	0.0000	0.9999	0.0001	0.0000	0.9991	0.0000	0.0000	0.0009
liv_19	0.0180	0.9820	0.0000	0.9995	0.0005	0.0000	0.9907	0.0000	0.0000	0.0094
liv_21	0.9910	0.0090	1.0000	0.0000	0.0000	0.9979	0.0000	0.0000	0.0022	0.0000
liv_25	0.9924	0.0076	1.0000	0.0000	0.0000	0.9993	0.0000	0.0000	0.0007	0.0000
liv_28	0.0096	0.9904	0.0000	0.9999	0.0001	0.0000	0.9991	0.0000	0.0000	0.0009
liv_31	0.9920	0.0080	1.0000	0.0000	0.0000	0.9989	0.0000	0.0000	0.0011	0.0000
liv_47	0.0150	0.9850	0.0000	0.9983	0.0017	0.0000	0.9900	0.0000	0.0000	0.0100
liv_48	0.9908	0.0092	1.0000	0.0000	0.0000	0.9982	0.0000	0.0000	0.0018	0.0000
liv_58	0.0080	0.9920	0.0000	0.9999	0.0001	0.0000	0.9996	0.0000	0.0000	0.0004
liv_61	0.0130	0.9870	0.0000	0.9993	0.0007	0.0000	0.9961	0.0000	0.0000	0.0039
liv_66	0.9910	0.0090	1.0000	0.0000	0.0000	0.9974	0.0000	0.0000	0.0026	0.0000
liv_70	0.9920	0.0080	1.0000	0.0000	0.0000	0.9988	0.0000	0.0000	0.0013	0.0000
liv_74	0.9911	0.0089	1.0000	0.0000	0.0000	0.9990	0.0000	0.0000	0.0010	0.0000
liv_76	0.9887	0.0113	1.0000	0.0000	0.0000	0.9985	0.0000	0.0000	0.0015	0.0000
liv_78	0.9685	0.0315	1.0000	0.0000	0.0000	0.9863	0.0000	0.0000	0.0137	0.0000
liv_80	0.9900	0.0100	1.0000	0.0000	0.0000	0.9974	0.0000	0.0000	0.0027	0.0000
liv_81	0.0110	0.9890	0.0000	0.9996	0.0004	0.0000	0.9972	0.0000	0.0000	0.0028
liv_87	0.9847	0.0153	0.9999	0.0000	0.0001	0.9958	0.0000	0.0000	0.0042	0.0000
lyo_59	0.9890	0.0110	1.0000	0.0000	0.0000	0.9992	0.0000	0.0000	0.0009	0.0000
lyo_71	0.9900	0.0100	1.0000	0.0000	0.0000	0.9978	0.0000	0.0000	0.0022	0.0000
lyo_80	0.9881	0.0119	1.0000	0.0000	0.0000	0.9955	0.0000	0.0000	0.0045	0.0000
lyo_83	0.9910	0.0090	1.0000	0.0000	0.0000	0.9986	0.0000	0.0000	0.0014	0.0000
mac_05	0.9930	0.0070	1.0000	0.0000	0.0000	0.9995	0.0000	0.0000	0.0005	0.0000
mac_23	0.9920	0.0080	1.0000	0.0000	0.0000	0.9992	0.0000	0.0000	0.0008	0.0000
mac_31	0.9920	0.0080	1.0000	0.0000	0.0000	0.9990	0.0000	0.0000	0.0010	0.0000
mac_33	0.9910	0.0090	1.0000	0.0000	0.0000	0.9981	0.0000	0.0000	0.0020	0.0000
mac_48	0.9920	0.0080	1.0000	0.0000	0.0000	0.9992	0.0000	0.0000	0.0008	0.0000
mac_60	0.9900	0.0100	1.0000	0.0000	0.0000	0.9995	0.0000	0.0000	0.0005	0.0000
mac_64	0.9920	0.0080	1.0000	0.0000	0.0000	0.9987	0.0000	0.0000	0.0013	0.0000
mac_66	0.9910	0.0090	1.0000	0.0000	0.0000	0.9981	0.0000	0.0000	0.0019	0.0000
mac_70	0.9870	0.0130	0.9998	0.0000	0.0002	0.9925	0.0000	0.0000	0.0075	0.0000
mac_75	0.9883	0.0117	0.9999	0.0000	0.0001	0.9943	0.0000	0.0000	0.0057	0.0000
mac_79	0.9910	0.0090	0.9999	0.0000	0.0001	0.9986	0.0000	0.0000	0.0014	0.0000
mac_86	0.9920	0.0080	1.0000	0.0000	0.0000	0.9990	0.0000	0.0000	0.0010	0.0000
mac_90	0.9910	0.0090	1.0000	0.0000	0.0000	0.9987	0.0000	0.0000	0.0013	0.0000
mon_01	0.9930	0.0070	1.0000	0.0000	0.0000	0.9997	0.0000	0.0000	0.0003	0.0000
mon_14	0.9837	0.0163	1.0000	0.0000	0.0000	0.9992	0.0000	0.0000	0.0009	0.0000
mon_37	0.0100	0.9900	0.0000	0.9998	0.0002	0.0000	0.9981	0.0000	0.0000	0.0019
mon_44	0.9940	0.0060	1.0000	0.0000	0.0000	0.9998	0.0000	0.0000	0.0002	0.0000
mon_62	0.9927	0.0073	1.0000	0.0000	0.0000	0.9993	0.0000	0.0000	0.0007	0.0000
mon_65	0.9910	0.0090	1.0000	0.0000	0.0000	0.9981	0.0000	0.0000	0.0019	0.0000
mon_67	0.9920	0.0080	1.0000	0.0000	0.0000	0.9990	0.0000	0.0000	0.0010	0.0000
mon_73	0.9890	0.0110	1.0000	0.0000	0.0000	0.9992	0.0000	0.0000	0.0008	0.0000
mon_75	0.9920	0.0080	1.0000	0.0000	0.0000	0.9993	0.0000	0.0000	0.0007	0.0000
mon_76	0.0070	0.9930	0.0000	1.0000	0.0000	0.0000	0.9997	0.0000	0.0000	0.0003
mon_77	0.9910	0.0090	1.0000	0.0000	0.0000	0.9991	0.0000	0.0000	0.0009	0.0000
mon_81	0.9516	0.0484	0.9994	0.0000	0.0006	0.9813	0.0000	0.0000	0.0187	0.0000
mon_83	0.9929	0.0071	1.0000	0.0000	0.0000	0.9993	0.0000	0.0000	0.0007	0.0000
mon_89	0.9940	0.0060	1.0000	0.0000	0.0000	0.9998	0.0000	0.0000	0.0003	0.0000

ora_05	0.9910	0.0090	1.0000	0.0000	0.0000	0.9976	0.0000	0.0000	0.0024	0.0000
ora_06	0.9920	0.0080	1.0000	0.0000	0.0000	0.9984	0.0000	0.0000	0.0016	0.0000
ora_09	0.9910	0.0090	1.0000	0.0000	0.0000	0.9984	0.0000	0.0000	0.0016	0.0000
ora_21	0.9553	0.0447	0.9997	0.0000	0.0003	0.9357	0.0000	0.0000	0.0643	0.0000
ora_23	0.9890	0.0110	1.0000	0.0000	0.0000	0.9957	0.0000	0.0000	0.0043	0.0000
ora_25	0.9868	0.0132	0.9996	0.0000	0.0004	0.9880	0.0000	0.0000	0.0120	0.0000
ora_27	0.9920	0.0080	1.0000	0.0000	0.0000	0.9992	0.0000	0.0000	0.0008	0.0000
ora_34	0.9879	0.0121	1.0000	0.0000	0.0000	0.9942	0.0000	0.0000	0.0058	0.0000
ora_42	0.9930	0.0070	1.0000	0.0000	0.0000	0.9996	0.0000	0.0000	0.0004	0.0000
ora_44	0.9920	0.0080	1.0000	0.0000	0.0000	0.9989	0.0000	0.0000	0.0011	0.0000
ora_46	0.9870	0.0130	0.9999	0.0000	0.0001	0.9977	0.0000	0.0000	0.0023	0.0000
ora_50	0.9851	0.0149	0.9998	0.0000	0.0002	0.9848	0.0000	0.0000	0.0152	0.0000
ora_60	0.9890	0.0110	1.0000	0.0000	0.0000	0.9970	0.0000	0.0000	0.0030	0.0000
ora_64	0.9914	0.0086	1.0000	0.0000	0.0000	0.9984	0.0000	0.0000	0.0016	0.0000
ora_69	0.9920	0.0080	1.0000	0.0000	0.0000	0.9991	0.0000	0.0000	0.0009	0.0000
ora_71	0.9790	0.0210	1.0000	0.0000	0.0000	0.9868	0.0000	0.0000	0.0132	0.0000
ora_74	0.9930	0.0070	1.0000	0.0000	0.0000	0.9996	0.0000	0.0000	0.0004	0.0000
ora_75	0.9930	0.0070	1.0000	0.0000	0.0000	0.9996	0.0000	0.0000	0.0004	0.0000
ora_76	0.9870	0.0130	0.9993	0.0000	0.0007	0.9908	0.0000	0.0000	0.0092	0.0000
ora_78	0.9930	0.0070	1.0000	0.0000	0.0000	0.9997	0.0000	0.0000	0.0003	0.0000
ora_83	0.9811	0.0189	1.0000	0.0000	0.0000	0.9862	0.0000	0.0000	0.0138	0.0000
ora_87	0.9439	0.0561	1.0000	0.0000	0.0000	0.9603	0.0000	0.0000	0.0397	0.0000
ora_90	0.9920	0.0080	1.0000	0.0000	0.0000	0.9988	0.0000	0.0000	0.0012	0.0000
pea_11	0.0361	0.9639	0.0000	0.9990	0.0010	0.0000	0.9219	0.0000	0.0000	0.0781
pea_15	0.0130	0.9870	0.0000	0.9997	0.0003	0.0000	0.9956	0.0000	0.0000	0.0044
pea_28	0.0082	0.9918	0.0000	1.0000	0.0000	0.0000	0.9990	0.0000	0.0000	0.0010
pea_31	0.0150	0.9850	0.0000	0.9994	0.0006	0.0000	0.9917	0.0000	0.0000	0.0084
pea_34	0.0090	0.9910	0.0000	1.0000	0.0000	0.0000	0.9994	0.0000	0.0000	0.0006
pea_51	0.0165	0.9835	0.0000	0.9980	0.0020	0.0000	0.9921	0.0000	0.0000	0.0079
pea_67	0.0127	0.9873	0.0000	0.9996	0.0004	0.0000	0.9883	0.0000	0.0000	0.0118
pea_69	0.0120	0.9880	0.0000	0.9988	0.0012	0.0000	0.9973	0.0000	0.0000	0.0027
pea_74	0.0090	0.9910	0.0000	0.9999	0.0001	0.0000	0.9993	0.0000	0.0000	0.0007
pea_82	0.0070	0.9930	0.0000	1.0000	0.0000	0.0000	0.9997	0.0000	0.0000	0.0003
pea_85	0.0170	0.9830	0.0000	0.9939	0.0061	0.0000	0.9884	0.0000	0.0000	0.0116
pea_87	0.0130	0.9870	0.0000	0.9979	0.0021	0.0000	0.9910	0.0000	0.0000	0.0090
tar_01	0.9897	0.0103	1.0000	0.0000	0.0000	0.9967	0.0000	0.0000	0.0033	0.0000
tar_03	0.9930	0.0070	1.0000	0.0000	0.0000	0.9997	0.0000	0.0000	0.0003	0.0000
tar_04	0.9920	0.0080	1.0000	0.0000	0.0000	0.9991	0.0000	0.0000	0.0009	0.0000
tar_06	0.9920	0.0080	1.0000	0.0000	0.0000	0.9988	0.0000	0.0000	0.0013	0.0000
tar_08	0.9761	0.0239	1.0000	0.0000	0.0000	0.9838	0.0000	0.0000	0.0162	0.0000
tar_12	0.9890	0.0110	0.9999	0.0000	0.0001	0.9937	0.0000	0.0000	0.0063	0.0000
tar_15	0.9930	0.0070	1.0000	0.0000	0.0000	0.9997	0.0000	0.0000	0.0003	0.0000
tar_17	0.9823	0.0177	0.9999	0.0000	0.0001	0.9828	0.0000	0.0000	0.0172	0.0000
tar_23	0.9920	0.0080	1.0000	0.0000	0.0000	0.9989	0.0000	0.0000	0.0011	0.0000
tar_32	0.9920	0.0080	1.0000	0.0000	0.0000	0.9990	0.0000	0.0000	0.0010	0.0000
tar_34	0.9911	0.0089	1.0000	0.0000	0.0000	0.9985	0.0000	0.0000	0.0015	0.0000
tar_37	0.9891	0.0109	1.0000	0.0000	0.0000	0.9970	0.0000	0.0000	0.0030	0.0000
tar_39	0.9915	0.0085	1.0000	0.0000	0.0000	0.9983	0.0000	0.0000	0.0017	0.0000
tar_42	0.9920	0.0080	1.0000	0.0000	0.0000	0.9992	0.0000	0.0000	0.0008	0.0000
tar_46	0.9920	0.0080	1.0000	0.0000	0.0000	0.9989	0.0000	0.0000	0.0011	0.0000
tar_48	0.9807	0.0193	1.0000	0.0000	0.0000	0.9755	0.0000	0.0000	0.0245	0.0000
tar_49	0.9930	0.0070	1.0000	0.0000	0.0000	0.9995	0.0000	0.0000	0.0005	0.0000
tar_50	0.9870	0.0130	0.9999	0.0000	0.0001	0.9909	0.0000	0.0000	0.0091	0.0000
tar_55	0.9930	0.0070	1.0000	0.0000	0.0000	0.9995	0.0000	0.0000	0.0005	0.0000
tar_56	0.9910	0.0090	1.0000	0.0000	0.0000	0.9982	0.0000	0.0000	0.0018	0.0000
tar_59	0.9910	0.0090	1.0000	0.0000	0.0000	0.9975	0.0000	0.0000	0.0025	0.0000
tar_67	0.9930	0.0070	1.0000	0.0000	0.0000	0.9991	0.0000	0.0000	0.0009	0.0000
tar_70	0.9810	0.0190	1.0000	0.0000	0.0000	0.9819	0.0000	0.0000	0.0181	0.0000
tar_75	0.9819	0.0181	0.9999	0.0000	0.0001	0.9903	0.0000	0.0000	0.0097	0.0000

tar_80	0.9930	0.0070	1.0000	0.0000	0.0000	0.9996	0.0000	0.0000	0.0004	0.0000
tar_86	0.9900	0.0100	1.0000	0.0000	0.0000	0.9959	0.0000	0.0000	0.0042	0.0000
tou_03	0.0220	0.9780	0.0000	0.9979	0.0021	0.0000	0.9524	0.0000	0.0000	0.0476
tou_09	0.0095	0.9905	0.0000	0.9999	0.0001	0.0000	0.9986	0.0000	0.0000	0.0014
tou_12	0.0220	0.9780	0.0000	0.9909	0.0091	0.0000	0.9854	0.0000	0.0000	0.0146
tou_15	0.0356	0.9644	0.0000	0.9870	0.0130	0.0000	0.9668	0.0000	0.0000	0.0332
tou_18	0.0079	0.9921	0.0000	1.0000	0.0000	0.0000	0.9998	0.0000	0.0000	0.0002
tou_21	0.0100	0.9900	0.0000	0.9996	0.0004	0.0000	0.9987	0.0000	0.0000	0.0013
tou_23	0.0120	0.9880	0.0000	0.9986	0.0014	0.0000	0.9943	0.0000	0.0000	0.0057
tou_27	0.0110	0.9890	0.0000	0.9994	0.0006	0.0000	0.9976	0.0000	0.0000	0.0024
tou_29	0.0240	0.9760	0.0000	0.9935	0.0065	0.0000	0.9684	0.0000	0.0000	0.0316
tou_33	0.0100	0.9900	0.0000	1.0000	0.0000	0.0000	0.9991	0.0000	0.0000	0.0010
tou_38	0.0339	0.9661	0.0000	0.9969	0.0031	0.0000	0.9494	0.0000	0.0000	0.0506
tou_42	0.0254	0.9746	0.0000	0.9917	0.0083	0.0000	0.9323	0.0000	0.0000	0.0677
tou_47	0.0130	0.9870	0.0000	0.9999	0.0001	0.0000	0.9932	0.0000	0.0000	0.0068
tou_49	0.0150	0.9850	0.0000	0.9993	0.0007	0.0000	0.9825	0.0000	0.0000	0.0175
tou_54	0.0325	0.9675	0.0000	0.9994	0.0006	0.0000	0.9681	0.0000	0.0000	0.0319
tou_56	0.0181	0.9819	0.0000	0.9957	0.0043	0.0000	0.9747	0.0000	0.0000	0.0253
tou_59	0.0090	0.9910	0.0000	0.9999	0.0001	0.0000	0.9993	0.0000	0.0000	0.0007
tou_66	0.0179	0.9821	0.0000	0.9975	0.0025	0.0000	0.9868	0.0000	0.0000	0.0132
tou_72	0.0322	0.9678	0.0000	0.9879	0.0121	0.0000	0.9400	0.0000	0.0000	0.0600
tou_75	0.0165	0.9835	0.0000	0.9997	0.0003	0.0000	0.9960	0.0000	0.0000	0.0040
tou_78	0.0110	0.9890	0.0000	0.9995	0.0005	0.0000	0.9956	0.0000	0.0000	0.0044
tou_80	0.0100	0.9900	0.0000	0.9995	0.0005	0.0000	0.9978	0.0000	0.0000	0.0023
tou_84	0.0110	0.9890	0.0000	0.9996	0.0004	0.0000	0.9954	0.0000	0.0000	0.0046
tou_86	0.0239	0.9761	0.0000	0.9956	0.0044	0.0000	0.9746	0.0000	0.0000	0.0254
tsr_07	0.0140	0.9860	0.0000	0.9997	0.0003	0.0000	0.9960	0.0000	0.0000	0.0040
tsr_09	0.0080	0.9920	0.0000	0.9999	0.0001	0.0000	0.9994	0.0000	0.0000	0.0006
tsr_11	0.0120	0.9880	0.0000	0.9989	0.0011	0.0000	0.9945	0.0000	0.0000	0.0056
tsr_24	0.0090	0.9910	0.0000	0.9998	0.0002	0.0000	0.9958	0.0000	0.0000	0.0042
tsr_41	0.0070	0.9930	0.0000	1.0000	0.0000	0.0000	0.9996	0.0000	0.0000	0.0004
tsr_45	0.0090	0.9910	0.0000	0.9998	0.0002	0.0000	0.9989	0.0000	0.0000	0.0011
tsr_52	0.0150	0.9850	0.0000	0.9977	0.0023	0.0000	0.9945	0.0000	0.0000	0.0055
tsr_60	0.0080	0.9920	0.0000	0.9999	0.0001	0.0000	0.9996	0.0000	0.0000	0.0004
val_01	0.9918	0.0082	1.0000	0.0000	0.0000	0.9990	0.0000	0.0000	0.0011	0.0000
val_10	0.9920	0.0080	0.9999	0.0000	0.0001	0.9991	0.0000	0.0000	0.0009	0.0000
val_23	0.9920	0.0080	1.0000	0.0000	0.0000	0.9986	0.0000	0.0000	0.0014	0.0000
val_25	0.9930	0.0070	1.0000	0.0000	0.0000	0.9994	0.0000	0.0000	0.0006	0.0000
val_62	0.9349	0.0651	0.9999	0.0000	0.0001	0.9536	0.0000	0.0000	0.0464	0.0000
val_64	0.9930	0.0070	1.0000	0.0000	0.0000	0.9994	0.0000	0.0000	0.0006	0.0000
val_70	0.9929	0.0071	1.0000	0.0000	0.0000	0.9991	0.0000	0.0000	0.0009	0.0000
val_78	0.9920	0.0080	1.0000	0.0000	0.0000	0.9993	0.0000	0.0000	0.0007	0.0000
val_83	0.9930	0.0070	1.0000	0.0000	0.0000	0.9996	0.0000	0.0000	0.0004	0.0000
val_85	0.9880	0.0120	0.9999	0.0000	0.0001	0.9986	0.0000	0.0000	0.0015	0.0000
val_90	0.9890	0.0110	1.0000	0.0000	0.0000	0.9983	0.0000	0.0000	0.0018	0.0000